Supporting Information for:

Homoleptic Nickel(II) Complexes of Redox-Tunable Pincer-type Ligands.

Jeewantha S. Hewage, Sarath Wanniarachchi, Tyler J. Morin, Brendan J. Liddle, Megan Banaszynski Sergey V. Lindeman, Brian Bennett, James R. Gardinier.

Table of Contents:

General Considerations. The compounds CuI, ^{t}BuONO, $CuBr_2$, CuI, M_2CO_3 (M = Na, K, Cs), *N*-Bromosuccinimide (NBS), Pd(acetate = $OAc)_2$, 2,2'-Bis(diphenylphosphino)-1,1'-binaphthyl (BINAP), 1-bromo-2-fluorobenzene, pyrazole, N,N'-dimethylethylenediamine (DMED), (Fc = ferrocenium)(BF_4), 4-cyanophenylboronic acid, 4-*tert*-butylphenylboronic acid, anhydrous DMF, $NiCl_2 \cdot 6H_2O$ and the 1.47 *M* [25% (w/w)] solution of (NEt_4)(OH) in CH_3OH were purchased commercially and used as received. The compounds HN(*p*-biphenyl^{t}Bu)$_2$,[S1] 1-(2-bromophenyl)-1H-pyrazole (BrPhpz),[S2] H(pzAn^{X}) (X = Me, H, CN, or CO_2Et; see Scheme 2),[S3] H(Me,Me),[S4] H(Me,H),[S2] H(Me,CF_3),[S2] H(CF_3,CF_3),[S2] and $Pd(PPh_3)_4$[S5] were prepared according to literature procedures. Dioxane, Et_2O, and THF were dried over sodium/benzophenone ketyl. Toluene, *p*-xylene, CH_2Cl_2, and CH_3CN were dried over CaH_2. Solvents used in reactions were distilled under argon prior to use.

Physical Measurements. Midwest MicroLab, LLC, Indianapolis, Indiana 45250, performed all elemental analyses. Melting point determinations were made on samples contained in glass capillaries using an Electrothermal 9100 apparatus and are uncorrected. ^{1}H, ^{13}C, and ^{19}F NMR spectra were recorded on a Varian 400 MHz spectrometer. Chemical shifts were referenced to solvent resonances at δ_H 7.27, δ_C 77.23 for $CDCl_3$. Abbreviations for NMR and UV-Vis br (broad), sh (shoulder), m (multiplet), ps (pseudo-), s (singlet), d (doublet), t (triplet), q (quartet), p (pentet), sept (septet). Electrochemical measurements were collected under a nitrogen atmosphere for samples as 0.1 m*M* solutions in CH_2Cl_2 with 0.1 M NBu_4PF_6 as the supporting electrolyte. A three-electrode cell comprised of an Ag/AgCl electrode (separated from the reaction medium with a semipermeable polymer membrane filter), a platinum working electrode, and a glassy carbon counter electrode was used for the voltammetric measurements. Data were collected at scan rates of 50, 100, 200, 300, 400, and 500 mV/s. With this set up, the

ferrocene/ferrocenium couple had an $E_{1/2}$ value of +0.52 V in CH_2Cl_2 at a scan rate of 200 mV/s, consistent with the literature values.[S6] Solid state magnetic susceptibility measurements were performed using a Johnson-Matthey MSB-MK1 instrument. Diamagnetic corrections were applied using tabulated values of Pascal's constants.[S7] Electronic absorption (UV-Vis/NIR) measurements were made on a Cary 5000 instrument. EPR spectra were obtained on both solid powder samples and as solutions ~0.2 m*M* in 1:1 CH_2Cl_2:toluene mixtures using a Bruker ELEXYS E600 equipped with an ER4116DM cavity resonating at 9.63 GHz, an Oxford instruments ITC503 temperature controller and a ESR-900 helium flow cryostat. The spectra were recorded using 100 kHz field modulation unless otherwise specified.

Ligand Precursor Syntheses.

2-Bromo-5-cyanophenyl-1H-pyrazole, Br-CNPhPz. A deep green solution of 2.4 mL (20.0 mmol) ^{t}BuONO and 2.23 g (10.0 mmol) $CuBr_2$ in 30 mL CH_3CN was purged with argon 20 min, then 1.85 g (10.0 mmol) H(pzAn^{CN}) was added as a solid. After the resulting violet solution had been heated at reflux 2 h, the mixture was added to 100 mL distilled H_2O. The resulting brown precipitate was collected by filtration and then was further purified by column chromatography on silica gel. Elution with 3:1 hexanes ethyl acetate (R_f 0.50) afforded 1.94 g (78%) of the desired compound as a pale yellow solid, after removing solvent and drying under vacuum. Mp, 114-116 ^{o}C. ^{1}H NMR ($CDCl_3$): δ_H 7.93 (d, *J* = 2.4 Hz, 1 H, H_5pz), 7.87 (d, *J* = 2.0 Hz, 1 H, H_3pz), 7.85 (d, *J* = 8.3 Hz, 1 H, Ar), 7.79 (d, *J* = 1.3 Hz, 1 H, Ar), 7.55 (dd, *J* = 8.3, 1.3 Hz, 1 H, Ar), 6.53 (dd, *J* = 2.4, 2.0 Hz, 1 H, H_4pz). ^{13}C NMR ($CDCl_3$): δ_C 142.1, 140.9, 135.3, 132.2, 131.6, 131.4, `23.6, 117.2, 112.8, 107.7. IR (KBr) ν_{CN} 2233 cm^{-1}.

2-Iodo-5-methylphenyl-1H-pyrazole, I-MePhPz. A solution of 3.18 g (46.1 mmol) $NaNO_2$ in 45 mL H_2O was slowly added to a cold (0^{o}C) solution of 5.32 g (30.7 mmol) H(pzAn^{Me}) in 100

mL 7 *M* H_2SO_4. After the solution had been stirred 15 min at 0°C, a solution of 7.65 g (46.1 mmol) KI in 25 mL H_2O was added slowly. After complete addition, the reaction mixture was heated at 80°C for 45 min using an external oil bath. The product mixture was neutralized with a 7 *M* KOH (aq) solution and then was extracted with three 50 mL portions of ethyl acetate. The combined organic fractions were dried over $MgSO_4$ and solvent was removed by rotary evaporation to leave a dark oily residue. The residue was subjected to column chromatography on silica gel. Solvent was removed from the second band (R_f 0.47) when eluting the column with 6:1 hexanes:ethyl acetate to give 5.91 g (68%) of the desired product as a brown oil of sufficient purity to be used successfully in subsequent coupling reactions. ^{1}H NMR ($CDCl_3$): δ_H 7.77 (d, *J* = 8.1 Hz, 1 H, Ar), 7.71 (d, *J* = 1.7 Hz, 1 H, H_3pz), 7.69 (d, *J* = 2.4 Hz, 1 H, H_5pz), 7.22 (d, *J* = 2.2 Hz, 1 H, Ar), 6.93 (dd, *J* = 8.1, 2.2 Hz, 1 H, Ar), 6.43 (dd, *J* = 2.4, 1.7 Hz, 1 H, H_5pz), 2.32 (s, 3 H, CH_3). ^{13}C NMR ($CDCl_3$): δ_C 143.2, 140.8, 139.7, 139.6, 131.24, 131.17, 129.0, 106.6, 89.9, 20.9.

3-bromo-4'-(1,1-dimethylphenyl)-*N*-(3-Bromo-4'-(1,1-dimethylphenyl)-[1,1'-biphenyl]-4-yl)-[1,1'-biphenyl]-4-amine, **HN(Br-biphenyl^{t}Bu)$_2$.** A solution of 0.45 mL (7.83 mmol) Br_2 dissolved in 30 mL of a 1:1 (v/v) mixture of MeOH:CH_2Cl_2 was added dropwise (1 mL/min) to a cold (0 °C), magnetically stirred solution of 1.69 g (3.91 mmol) HN(*p*-biphenyl^{t}Bu)$_2$ in 150 mL of a 1:1 (v/v) mixture of MeOH:CH_2Cl_2. After the resulting orange solution had been stirred 1 h at 0 °C, 150 mL of a saturated $Na_2S_2O_3$ solution was added whereupon the orange color disappeared. The aqueous and organic layers were separated. The aqueous layer was extracted with two 25 mL portions CH_2Cl_2. The combined organic layers were dried over $MgSO_4$, filtered and solvent was removed by vacuum distillation to leave a dark oil. The oil was subject to flushed through a short pad of silica gel using 4:1 hexanes:CH_2Cl_2 (R_f 0.65) as an eluent.

Removal of solvent by vacuum distillation gave 1.66 g (70%) of the desired product as a colorless crystalline solid. Mp, 138-140 °C. ^{1}H NMR ($CDCl_3$) δ_H 7.86 (d, J = 2 Hz, 2 H), 7.47 (m, 12 H, Ar), 6.56 (br s, 1 H, NH), 1.39 (s, 18 H, CH_3). ^{13}C NMR ($CDCl_3$) δ_C 150.5, 138.9, 136.6, 135.7, 131.6, 126.7, 131.6, 126.7, 126.4, 125.9, 118.1, 114.6, 34.7, 31.5.

Ligand Syntheses.

H(H,H). A Schlenk flask charged with 3.18 g (20.0 mmol) H(pzAn^{H}), 4.45 g (20.0 mmol) BrPhpz, 7.80 g (23.9 mmol) Cs_2CO_3 was deoxygenated by three evacuation and argon back-fill cycles. Next, 15 mL dry, argon-purged dioxane was added by syringe and then 0.762 g (4.00 mmol) CuI was added as a solid under an argon blanket. After the reaction mixture had been heated at reflux for 15 h under argon, it was cooled to room temperature. Dioxane was removed by vacuum distillation. The solid residue was dissolved in a mixture of 50 mL ethyl acetate and 100 mL H_2O. The aqueous and organic layers were separated. The aqueous fraction was extracted with three 30 mL portions of ethyl acetate. The combined organic fractions were dried over $MgSO_4$, filtered, and solvent was removed under vacuum by rotary evaporation to leave a brown oily residue. The residue was then subjected to column chromatography on silica gel. A beige solid mixture (4.5 g) of the desired product along with a trace of H(pzAn^{H}) was obtained by collecting the second band (R_f 0.56) when eluting with 8:1 hexanes:ethyl acetate and removing solvent under vacuum. The H(pzAn^{H}) impurity was removed by washing with EtOH in the following manner. A 20 mL aliquot of absolute EtOH was added to the 4.5 g beige solid mixture, the mixture dissolved on heating to reflux 2 min. The orange solution was cooled to room temperature which deposited 3.81 g (63 %) colorless crystals of pure H(HH) that were collected by filtration and dried under vacuum. An additional crop of crystals (0.300 g, 5 %) was obtained by cooling the mother liquor to -30 °C for 15 h, filtering, and drying under vacuum.

Total yield of pure H(HH) as colorless prism crystals: 4.11 g (68 %). Mp, 124 - 126 °C. ^{1}H NMR ($CDCl_3$): δ_H 8.77 (s, 1 H, NH), 7.72 (d, *J* = 2 Hz, 2 H, H_5pz), 7.71 (d, *J* = 2 Hz, 2 H, H_3pz), 7.46 (dd, *J* = 8, 1 Hz, 2 H, Ar), 7.32 (dd, *J* = 8, 1 Hz, 2 H, Ar), 7.23 (td, *J* = 8, 1 Hz, 2 H, Ar), 6.96 (td, *J* = 8, 1 Hz, 2 H, Ar), 6.44 (pst, *J* = 2 Hz, 2 H, H_4pz). ^{13}C NMR ($CDCl_3$): δ_C 140.8, 137.1, 130.4, 130.1, 128.4, 125.5, 121.1, 118.7, 106.9.

H(Me,Br). A solution of 0.548 g (3.08 mmol) NBS in 20 mL CH_3CN was added dropwise to a cold (0 °C) solution of 0.971 g (3.08 mmol) H(Me,H) in 20 mL CH_3CN. After the mixture had been stirred at 0°C 2 h, a 10 mL aliquot of saturated aqueous $Na_2S_2O_3$ solution was added. The aqueous and organic layers were separated. The aqueous layer was extracted with three 10 mL portions ethyl acetate. The combined organic layers were washed with a saturated aqueous Na_2CO_3 solution, and then were dried over $MgSO_4$, filtered, and volatiles were removed under vacuum to leave an oily residue. The residue was subjected to column chromatography on silica gel using 4:1 hexanes:ethyl acetate as the eluent. The desired product (0.969 g, 80%) was isolated as a colorless solid after removing solvent from the band near the solvent front (R_f 0.8). Mp, 105 – 107 °C. ^{1}H NMR ($CDCl_3$): δ_H 8.70 (s, 1 H, NH), 7.79 (d, *J* = 1.6 Hz, 1 H, pz), 7.73 (d, *J* = 2.4 Hz, 1 H, pz), 7.71 (d, *J* = 2.4 Hz, 1 H, pz), 7.69 (d, *J* = 1.7 Hz, 1 H, pz), 7.43 (d, *J* = 2.2 Hz, 1 H, Ar), 7.32 (d, *J* = 8.3 Hz, 1 H, Ar), 7.27 (dd, *J* = 8.8, 2.2 Hz, 1 H, Ar), 7.21 (s, 1 H, Ar), 7.19 (d, *J* = 6.7 Hz, 1 H, Ar), 7.08 (dd, *J* = 8.1, 1.5 Hz, 1 H, Ar), 6.47 (pst, *J* = 2.1 Hz, 1 H, pz), 6.41 (pst, *J* = 2.3 Hz, 1 H, pz), 2.35 (s, 3 H, CH_3). ^{13}C NMR ($CDCl_3$): δ_C 141.1, 140.7, 137.1, 133.2, 132.3, 131.4, 131.1, 130.3, 130.1, 130.0, 129.0, 127.8, 126.0, 120.6, 118.6, 111.1, 107.2, 106.9, 20.8.

H(Me,CO_2Et). In an argon-filled drybox, a Schlenk flask was charged with 1.02 g (4.39 mmol) H(pzAn^{CO_2Et}), 1.72 g (5.27 mmol) Cs_2CO_3, 0.059 g (0.26 mmol) $Pd(OAc)_2$, and 0.109 g (0.176 mmol) BINAP. The flask was removed from the drybox and was attached to a Schlenk line. A solution of 1.50 g (5.27 mmol) I-MePhPz in 20 mL toluene was purged with argon 20 min and then was transferred via cannula to the reaction flask containing aniline, base, and catalyst. After the reaction mixture had been heated at reflux 3 d, toluene was removed by vacuum distillation. The residue was dissolved in a biphasic mixture of 50 mL distilled water and 50 mL ethyl acetate. The organic and aqueous phases were separated. The aqueous phase was extracted with two 50 mL portions ethyl acetate. The combined organic layers were dried over $MgSO_4$, filtered, and solvent was removed by rotary evaporation to leave an oily residue. The residue was subjected to column chromatography on silica gel using 4:1 hexanes:ethyl acetate as the eluent. The desired product 1.24 g (73%) was obtained as a pale yellow gum after removing solvent from the third band (R_f 0.4). ^{1}H NMR ($CDCl_3$): δ_H 9.15 (s, 1 H, NH), 7.94 (d, *J* = 2.5 Hz, 1 H, pz), 7.83 (d, *J* = 8.5 Hz, 1 H, Ar), 7.79 (d, *J* = 2.5 Hz, 1 H, pz), 7.77 (d, *J* = 2.1 Hz, 1 H, pz), 7.71 (d, *J* = 3.0 Hz, 1 H, pz), 7.67 (s, 1 H, Ar), 7.44 (d, *J* = 8.3 Hz, 1 H, Ar), 7.27 (s, 1 H, Ar), 7.26 (d, *J* = 8.1 Hz, 1 H, Ar), 7.14 (d, *J* = 8.2 Hz, 1 H, Ar), 6.51 (pst, *J* = 3.1 Hz, 1 H, pz), 6.39 (pst, *J* = 3.0 Hz, 1 H, pz), 4.34 (q, *J* = 7.1 Hz, 2 H, CH_2), 2.38 (s, 3 H, Ar-CH_3), 1.37 (t, *J* = 7.1 Hz, 3 H, Et-CH_3). ^{13}C NMR ($CDCl_3$): δ_C 166.1, 142.6, 141.1, 140.8, 133.9, 132.7, 131.9, 130.3, 130.2, 130.0, 129.0, 127.6, 126.5, 126.1, 122.7, 120.9, 114.6, 107.1, 107.0, 60.9, 20.9, 14.6. IR (KBr) ν_{CO} 1706 cm^{-1}.

H(Br,Br). A solution of 1.20 g (6.76 mmol) NBS in 45 mL CH_3CN was added dropwise to a cold (0 ^{o}C) solution of 1.02 g (3.38 mmol) H(H,H) in 30 mL CH_3CN. After complete addition, the mixture was stirred at 0 ^{o}C until the solution noticeably darkened (ca. 1 h). Then, 50 mL of a

saturated $Na_2S_2O_3$ solution was added. The biphasic mixture was poured into 100 mL H_2O and the layers were separated. The aqueous layer was extracted with three 50 mL portions ethyl acetate. The combined organic layers were washed with 20 mL of saturated Na_2CO_3 solution, dried over $MgSO_4$, and filtered. Solvent was removed by vacuum distillation to leave an oily residue that was subjected to column chromatography on silica gel using 6:1 hexanes:ethyl acetate as the eluent. The desired product (1.26 g, 82 %) was isolated as a colorless solid after removing solvent from the second band (R_f 0.62). Mp, 95-97 °C. ^{1}H NMR ($CDCl_3$): δ_H 9.04 (s, 1 H, NH), 7.73 (m, 4 H, pz), 7.48 (d, J = 2.2 Hz, 2 H, Ar), 7.33 (dd, J = 8.8, 2.2 Hz, 2 H, Ar), 7.27 (d, J = 8.8 Hz, 2 H, Ar), 6.47 (pst, J = 2.1 Hz, 2 H, pz). ^{13}C NMR ($CDCl_3$): δ_C 141.1, 135.6, 131.1, 130.0, 127.9, 120.1, 112.7, 107.4.

H(Me,CN). Under an argon atmosphere a Schlenk flask was charged with 0.759 g (4.12 mmol) H(pzAn^{CN}), 1.61 g (4.94 mmol) Cs_2CO_3, 0.0585 g (0.261 mmol) $Pd(OAc)_2$, 0.135 g (0.217 mmol) BINAP. A solution of 1.29 g (4.53 mmol), I-MePhPz in 15 mL dry toluene was purged with argon 15 min and then was transferred via cannula to the flask containing the base and catalyst mixture. The reaction mixture was heated at reflux 48 h under argon. After cooling to room temperature toluene was removed by vacuum distillation. The solid product mixture was dissolved in a biphasic mixture of 50 mL H_2O and 50 mL ethyl acetate. The aqueous and organic layers were separated. The aqueous layer was extracted with two 50 mL portions of ethyl acetate. The combined organic layers were dried over $MgSO_4$, filtered, and volatiles were removed under vacuum by rotary evaporation. The remaining brown oil was subjected to column chromatography on silica gel using 1:2 Et_2O:hexane. A 0.719 g (51%) sample of pure H(Me,CN) as a colorless solid was obtained after removing solvent from the second band (R_f 0.52) and drying under vacuum. Mp, 93-94 °C. ^{1}H NMR ($CDCl_3$): δ_H 9.31 (s, 1 H, NH), 7.80

(d, J = 1.4 Hz, 1 H, pz), 7.74 (d, J = 1.9 Hz, 1 H, pz), 7.70 (d, J = 2.4 Hz, 1 H, pz), 7.65 (d, J = 1.4 Hz, 1 H, pz), 7.51 (d, J = 1.9 Hz, Ar), 7.40 (d, J = 8.1 Hz, 1 H, Ar), 7.38 (dd, J = 8.6, 1.9 Hz, 1 H, Ar), 7.28 (d, J = 1.4 Hz, 1 H, Ar), 7.23 (d, J = 8.7 Hz, 1 H, Ar), 7.16 (dd, J = 8.2, 1.8 Hz, 1 H, Ar), 6.53 (dd, J = 2, 1 Hz, 1 H, pz), 6.39 (dd, J = 2, 1 Hz, 1 H, pz), 2.39 (s, 3 H, CH_3). ^{13}C NMR ($CDCl_3$): δ_C 142.7, 141.5, 140.9, 134.9, 133.1, 132.5, 131.0, 130.2, 129.8, 129.1, 128.5, 127.8, 126.1, 123.4, 119.2, 115.2, 107.6, 107.2, 101.0, 21.0. IR (KBr) ν_{CN} 2225 cm^{-1}.

H(CN,CN). A Schlenk flask was charged with 0.755 g (4.10 mmol) H(pzAn^{CN}), 1.017 g (4.10 mmol) Br-CNPhPz, 1.603 g (4.92 mmol) Cs_2CO_3 and then was deoxygenated by three evacuation and argon back-fill cycles. Next, 15 mL of argon-purged, dry dioxane was added by syringe and then 0.156 g (0.820 mmol) CuI was added under an argon blanket. After the reaction mixture had been heated at reflux 15 h under argon, it was cooled to room temperature and dioxane was removed by vacuum distillation. The resulting solid was dissolved in a biphasic mixture of 50 mL H_2O and 50 mL ethyl acetate. The aqueous and organic fractions were separated. The aqueous fraction was extracted with three 30 mL portions ethyl acetate. The combined organic fractions were dried over $MgSO_4$, filtered and volatiles were removed under vacuum with the aid of a rotary evaporator. The resulting brown oil was subjected to column chromatography on silica gel using 1:1 ethyl acetate:hexanes. The desired product was obtained as a yellowish solid after removing solvent from the second band (R_f 0.37). Recrystallization by cooling a boiling absolute ethanol solution to room temperature over the course of hours and then to -30 ^oC overnight afforded 0.72 g (50%) H(CN,CN) as pale yellow crystals. Mp, 178-180 ^oC. ^1H NMR ($CDCl_3$): δ_H 10.32 (s, 1 H, NH), 7.79 (d, J = 1.9 Hz, 2 H, H_3pz), 7.77 (d, J = 2.5 Hz, H_5pz), 7.64 (d, J = 1.6 Hz, 2 H, Ar), 7.56 (s, 2 H, Ar), 7.55 (d, J = 1.6 Hz, Ar), 6.55 (dd, J =

2.5, 1.9 Hz, 2 H, H_4pz). ^{13}C NMR ($CDCl_3$): δ_C 141.8, 139.5, 132.2, 130.5, 130.1, 128.8, 118.9, 118.3, 108.1, 104.9. IR (KBr) ν_{CN} 2226 cm^{-1}.

H(^{tBu}Ph,^{tBu}Ph). *Method A.* In an argon-filled drybox, a Schlenk flask was charged with 0.408 g (0.889 mmol) H(Br,Br), 0.475 g (2.67 mmol), 4-*tert*-butylphenylboronic acid, and 0.206 g (0.178 mmol) $Pd(PPh_3)_4$. The flask was removed from the drybox and attached to a Schlenk line. A solution of 30 mL C_6H_6 and 10 mL absolute ethanol was purged with argon 15 min and was transferred to the reaction flask under argon via cannula. Next, 10 mL of an argon-purged 2 *M* aqueous Na_2CO_3 solution was transferred via cannula to the reaction flask. After the magnetically-stirred biphasic mixture had been heated at 80°C for 16 h with the aid of an external oil bath, the mixture was cooled to room temperature and poured into 100 mL H_2O. The aqueous and organic fractions were separated. The aqueous layer was extracted with two 50 mL portions ethyl acetate. The combined organic layers were dried over $MgSO_4$ and filtered. The oily residue that was obtained after removing solvents under vacuum was subjected to column chromatography on silica gel using 1:6 ethyl acetate:hexanes as the eluent. The desired product (0.383 g, 76%) H(^{tBu}Ph,^{tBu}Ph) was obtained as a colorless solid after removing solvent from the second band (R_f 0.45) and drying under vacuum 1 h.

Method B. A Schlenk flask charged with 2.61 g (4.41 mmol) HN(Br-biphenyl^{t}Bu)$_2$ 1.06 g (15.4 mmol) pyrazole, 2.16 g (15.4 mmol) K_2CO_3 and 0.19 mL (0.16 g, 1.8 mmol) DMED was deoxygenated by three evacuation and argon back-fill cycles. A 10 mL aliquot of dry, distilled, and argon-purged *p*-xylenes was added by syringe. Then, 0.0840 g (0.441 mmol) CuI was added under an argon blanket. After the resulting mixture had been heated at reflux 3 d under argon, the mixture was cooled to room temperature. Then 30 mL each H_2O and CH_2Cl_2 were added to dissolve the solids. The aqueous and organic layers were separated. The aqueous layer was

extracted with three 25 mL portions CH_2Cl_2. The combined organic layers were dried over $MgSO_4$ and filtered. Volatiles were removed under vacuum to give a dark oil. The oil was subjected to flash chromatography on silica gel. First, elution with hexanes removed residual xylene. Then, elution with 8:1 hexane:ethyl acetate afforded 1.22 g (49 %) of H(^{tBu}Ph,^{tBu}Ph) as a colorless solid after removing solvent from the second band (R_f 0.39) and drying under vacuum. Mp, 138-140 °C. ^{1}H NMR ($CDCl_3$): δ_H 8.94 (s, 1 H, NH), 7.78 (d, J = 2.4 Hz, 2 H, H_5pz), 7.77 (d, J = 1.7 Hz, 2 H, H_3pz), 7.59 (d, J = 6.4 Hz, 2 H, Ar), 7.58 (s, 2 H, Ar), 7.53 (d, J = 8.5 Hz, 4 H, Ar), 7.51 (dd, J = 8.7, 2.2 Hz, 2 H, Ar), 7.47 (d, J = 8.5 Hz, 4 H, Ar), 6.49 (dd, J = 2.4, 1.7 Hz, 2 H, H_4pz), 1.37 (s, 18 H, CH_3). ^{13}C NMR ($CDCl_3$): δ_C 150.4, 140.9, 137.2, 136.0, 134.1, 130.7, 130.2, 126.8, 126.4, 126.0, 123.8, 119.0, 107.0, 34.7, 31.6.

H(^{CN}Ph,^{CN}Ph). In an argon-filled drybox, a Schlenk flask was charged with 0.252 g (0.548 mmol) H(Br,Br), 0.242 g (1.64 mmol), 4-cyanophenyl boronic acid, and 0.127 g (0.110 mmol) $Pd(PPh_3)_4$. The flask was removed from the drybox and attached to a Schlenk line. A solution of 15 mL C_6H_6 and 5 mL absolute ethanol was purged with argon 15 min and was transferred to the reaction flask under argon via cannula. Next, 5 mL of an argon-purged 2 *M* aqueous Na_2CO_3 solution was transferred via cannula to the reaction flask. After the magnetically-stirred biphasic mixture had been heated at 80°C for 16 h with the aid of an external oil bath, the mixture was cooled to room temperature and poured into 100 mL H_2O. The aqueous and organic fractions were separated. The aqueous layer was extracted with three 50 mL portions ethyl acetate. The combined organic layers were dried over $MgSO_4$ and filtered. The oily residue that was obtained after removing solvents under vacuum was subjected to column chromatography on silica gel using 1:1 ethyl acetate:hexanes as the eluent. The product which eluted in the pale pink-orange band (R_f 0.39) was recrystallized from absolute ethanol to give 0.146 g (53%) H(^{CN}Ph,^{CN}Ph) as a

yellow solid. Mp, 200-202 ºC. ^{1}H NMR ($CDCl_3$): δ_H 9.28 (s, 1 H, NH), 7.82 (d, *J* = 2.4 Hz, 2 H, H_5pz), 7.79 (d, *J* = 1.7 Hz, 2 H, H_3pz), 7.73 (d, *J* = 8.4 Hz, 4H, Ar), 7.68 (d, *J* = 8.4 Hz, 4 H, Ar), 7.62 (d, *J* = 8.9 Hz, 2 H, Ar), 7.61 (d, *J* = 2.2 Hz, 2 H, Ar), 7.53 (dd, *J* = 8.9, 2.3 Hz, 2 H, Ar), 6.53 (dd, *J* = 2.4, 1.7 Hz, 2H, H_4pz). ^{13}C NMR ($CDCl_3$): δ_C 144.2, 141.3, 137.0, 132.9, 132.2, 130.9, 130.2, 127.2, 127.1, 124.2, 119.2, 119.1, 110.9, 107.4. IR (KBr) ν_{CN} 2227 cm^{-1}.

Nickel Complex Syntheses. Except where noted, the following compounds were prepared in a manner similar to that described in the main text for Ni(Me,Me)$_2$ (**1**) where the heating time, amount of solvent, and subsequent work-up procedure were identical to that described for **1**. The amounts of ligand, nickel salt, and base that were used varied in the preparation of each complex and are given below along with the yield and characterization data.

Ni(Me,H)$_2$·0.5H$_2$O, 2·0.5H$_2$O. A mixture of 0.447 g (1.42 mmol) H(Me,H), 0.169 g (0.709 mmol) $NiCl_2·6H_2O$, and 1.4 mmol (NEt_4)(OH) (0.97 mL of a 1.47 *M* solution in MeOH) gave 0.430 g (87%) **2**·0.5H_2O as a yellow-brown powder after collecting by filtration, washing with hexanes, and heating at 80ºC under vacuum 4 h. Mp, >350ºC. Anal. Calcd. (found) for $C_{38}H_{33}N_{10}NiO_{0.5}$: C, 65.54 (65.36); H, 4.78 (4.91); N, 20.11 (19.88). μ_{eff} (solid, 295 K) = 2.7 μ_B. UV-Vis (CH_2Cl_2) λ_{max}, nm (ε, $M^{-1}cm^{-1}$): 243 (50,500), 365 (31,800), 408 sh (14,000), 456 sh (640), 541 (180), 791 sh (77), 868 (110). Samples that were collected and washed as above but then were air-dried rather than heated under vacuum analyzed as **2**·1.5CH_2Cl_2·0.5H_2O, Anal. Calcd. (found) for $C_{39.5}H_{36}Cl_3N_{10}NiO_{0.5}$: C, 57.59 (57.70); H, 4.40 (4.67); N, 17.00 (17.05).

Ni(H,H)$_2$·H$_2$O, 3·H$_2$O. A mixture of 0.204 g (0.675 mmol) H(H,H), 0.0803 g (0.338 mmol) $NiCl_2·6H_2O$, and 0.68 mmol (NEt_4)(OH) (0.46 mL of a 1.47 *M* solution in MeOH) gave 0.187 g (82%) **3** H_2O as a tan solid. Mp, >350ºC. Anal. Calcd. (found) for $C_{36}H_{30}N_{10}NiO$: C, 63.83

(63.57); H, 4.78 (4.91); N, 20.68 (20.49). μ_{eff} (solid, 295 K) = 3.2 μ_B. UV-Vis (CH_2Cl_2) λ_{max}, nm (ε, $M^{-1}cm^{-1}$): 243 (48,000), 364 (30,100), 401 (14,400), 447 sh (760), 538 (166), 798 sh (77), 872 (113). Crystals of **3**·CH_2Cl_2 suitable for single crystal X-ray diffraction were grown by layering a CH_2Cl_2 solution of **3** H_2O with hexane and allowing solvents to diffuse.

Ni(Me,Br)$_2$, 4. A mixture of 0.343 g (0.869 mmol) H(Me,Br), 0.103 g (0.435 mmol) $NiCl_2·6H_2O$, and 0.87 mmol (NEt_4)(OH) (0.59 mL of a 1.47 *M* solution in MeOH) gave 0.355 g (97%) **4** as an orange-brown solid. Mp, 320ºC dec. to black liq. Anal. Calcd. (found) for $C_{38}H_{30}N_{10}Br_2Ni$: C, 54.00 (53.69); H, 3.58 (3.67); N, 16.57 (16.37). μ_{eff} (solid, 295 K) = 2.8 μ_B. UV-Vis (CH_2Cl_2) λ_{max}, nm (ε, $M^{-1}cm^{-1}$): 247 (59,300), 369 (43,000), 410 sh (15,500), 460 sh (725), 539 (214), 794 sh (72), 870 (120). Crystals suitable for single crystal X-ray diffraction were grown by layering a CH_2Cl_2 solution with hexane and allowing solvents to diffuse.

Ni(Me,CO$_2$Et)$_2$ 2MeOH, 5 2MeOH. A mixture of 0.500 g (1.29 mmol) H(Me,CO_2Et), 0.153 g (0.645 mmol) $NiCl_2·6H_2O$, and 1.29 mmol (NEt_4)(OH) (0.88 mL of a 1.47 *M* solution in MeOH) gave 0.566 g (98%) **5 2MeOH** as a dark orange solid. Mp, 330ºC dec. to black liq. Anal. Calcd. (found) for $C_{46}H_{48}N_{10}NiO_6$: C, 61.69 (61.34); H, 5.40 (5.13); N, 15.64 (15.78). μ_{eff} (solid, 295 K) = 2.8 μ_B. IR (KBr) $\nu_{C=O}$ 1699 cm^{-1}. UV-Vis (CH_2Cl_2) λ_{max}, nm (ε, $M^{-1}cm^{-1}$): 240 (53,500), 300 (9,800), 356 sh (17,400), 399 (50,100), 490 sh (510), 529 (430), 798 sh (122), 869 (154).

Ni(Me,CF$_3$)$_2$, 6. A mixture of 0.489 g (1.28 mmol) H(Me,CF_3), 0.152 g (0.638 mmol) $NiCl_2·6H_2O$, and 1.28 mmol (NEt_4)(OH) (0.87 mL of a 1.47 *M* solution in MeOH) gave 0.417 g (97%) **6** as an orange-brown solid. Mp, 345ºC dec. to black liq. Anal. Calcd. (found) for $C_{40}H_{30}N_{10}F_6Ni$: C, 58.35 (57.98); H, 3.67 (3.72); N, 17.01 (16.88). μ_{eff} (solid, 295 K) = 2.9 μ_B. UV-Vis (CH_2Cl_2) λ_{max}, nm (ε, $M^{-1}cm^{-1}$): 246 (54,700), 377 (36,200), 453 sh (570), 536 (190),

798 sh (78), 871 (120). Crystals suitable for single crystal X-ray diffraction were grown by layering a CH_2Cl_2 solution with hexane and allowing solvents to diffuse. A sample that was collected and washed with Et_2O but then was air-dried rather than heated under vacuum analyzed as **6**·H_2O, Anal. Calcd. (found) for $C_{40}H_{32}F_6N_{10}NiO$: C, 57.10 (56.84); H, 3.83 (3.75); N, 16.65 (16.55).

Ni(Br,Br)$_2$, 7. A mixture of 0.242 g (0.526 mmol) H(Br,Br), 0.0625 g (0.263 mmol) $NiCl_2·6H_2O$, and 0.529 mmol (NEt_4)(OH) (0.36 mL of a 1.47 *M* solution in MeOH) gave 0.219 g (85%) **7** as an orange-brown solid. Mp, >350°C. Anal. Calcd. (found) for $C_{36}H_{24}N_{10}Br_4Ni$: C, 44.35 (44.43); H, 2.48 (2.59); N, 14.37 (14.22). μ_{eff} (solid, 295 K) = 3.0 μ_B. UV-Vis (CH_2Cl_2) λ_{max}, nm (ε, $M^{-1}cm^{-1}$): 247 (63,400), 373 (48,100), 463 sh (650), 536 (250), 788 sh (78), 873 (140).

Ni(Me,CN)$_2$, 8. A mixture of 0.302 g (0.887 mmol) H(Me,CN), 0.105 g (0.443 mmol) $NiCl_2·6H_2O$, and 0.89 mmol (NEt_4)(OH) (0.61 mL of a 1.47 *M* solution in MeOH) gave 0.288 g (88%) **8** as an orange-brown solid. Mp, >350°C. Anal. Calcd. (found) for $C_{40}H_{30}N_{12}Ni$: C, 65.15 (64.97); H, 4.10 (4.20); N, 22.79 (22.69). μ_{eff} (solid, 295 K) = 2.9 μ_B. IR (KBr) ν_{CN} 2206 cm^{-1}. λ_{max}, nm (ε, $M^{-1}cm^{-1}$): 238 (75,500), 293 sh (13,300), 388 (57,600), 473 sh (580), 520 (410), 790 sh (130), 877 (195). X-ray quality crystals of **8** were grown by layering hexanes over a CH_2Cl_2 solution and allowing solvents to diffuse 2 d. A sample that was collected and washed with Et_2O but then was air-dried rather than heated under vacuum analyzed as **8**·0.5H_2O, Anal. Calcd. (found) for $C_{40}H_{31}N_{12}NiO_{0.5}$: C, 64.36 (64.40); H, 4.19 (4.07); N, 22.52 (22.31).

Ni(CF_3,CF_3)$_2$, 9. A mixture of 0.413 g (0.943 mmol) H(CF_3,CF_3), 0.112 g (0.472 mmol) $NiCl_2·6H_2O$, and 0.94 mmol (NEt_4)(OH) (0.64 mL of a 1.47 *M* solution in MeOH) gave 0.410 g

(93%) **9** as a dark orange solid after filtration, washing with hexanes and drying at 80°C under vacuum 4 h. Mp, >350°C. Anal. Calcd. (found) for $C_{40}H_{24}N_{10}F_{12}Ni$: C, 51.58 (51.38); H, 2.60 (2.80); N, 15.04 (14.85). μ_{eff} (solid, 295 K) = 3.1 μ_B. λ_{max}, nm (ε, $M^{-1}cm^{-1}$): 244 (56,000), 282 sh (11,100), 347 sh (23,600), 382 (51,500), 448 sh (670), 527 (210), 794 sh (55), 880 (120). Anal. Calcd. (found) for $C_{40}H_{24}N_{10}F_{12}Ni$: C, 51.58 (51.38); H, 2.60 (2.80); N, 15.04 (14.85). A sample that was collected and washed as above but then was air-dried rather than heated under vacuum analyzed as **9**·0.5H_2O, Anal. Calcd. (found) for $C_{40}H_{25}N_{10}NiO_{0.5}$: C, 51.09 (51.14); H, 2.68 (2.73); N, 14.72 (14.89).

Ni(CN,CN)$_2$ 0.5H_2O, 10 0.5H_2O. Owing the relatively lower solubility of the ligand in MeOH versus other ligands, the mixture of 0.240 g (0.682 mmol) H(CN,CN), 0.0810 g (0.341 mmol) $NiCl_2·6H_2O$, and 0.68 mmol (NEt_4)(OH) (0.46 mL of a 1.47 *M* solution in MeOH) was heated at reflux 6h and was filtered hot. After washing with Et_2O and drying under vacuum 0.225 g (86%) **10** 0.5H_2O as an orange-brown solid was obtained. Mp, >350°C. Anal. Calcd. (found) for $C_{40}H_{25}N_{14}NiO_{0.5}$: C, 62.52 (62.60); H, 3.28 (3.34); N, 25.52 (25.56). μ_{eff} (solid, 295 K) = 3.2 μ_B. IR (KBr) ν_{CN} 2214 cm^{-1}. λ_{max}, nm (ε, $M^{-1}cm^{-1}$): 242 (99,200), 303 (22,300), 346 (27,300), 407 (118,000), 491 (930), 512 (982), 792 sh (81), 841 (159) , 893 (160). A mixture of X-ray quality dark red-brown blocks of **10**·2acetone and red prisms of **10**·acetone were grown by layering an acetone solution of **10** 0.5H_2O with hexane and allowing solvents to diffuse over 1d.

Ni(^{tBuPh}Ph,^{tBuPh}Ph)$_2$, 11. A mixture of 0.339 g (0.599 mmol) H(^{tBu}Ph,^{tBu}Ph), 0.0712 g (0.300 mmol) $NiCl_2·6H_2O$, and 0.60 mmol (NEt_4)(OH) (0.41 mL of a 1.47 *M* solution in MeOH) gave 0.339 g (95%) **11** as an orange-brown solid after filtration, washing with hexanes, and heating at 80°C under vacuum 8h. Mp, 345°C dec. to black liq. Anal. Calcd. (found) for $C_{76}H_{76}N_{10}Ni$: C, 76.83 (76.68); H, 6.45 (6.51); N, 11.79 (11.85). μ_{eff} (solid, 295 K) = 2.8 μ_B. λ_{max}, nm (ε, $M^{-1}cm^{-}$

^{1}): 250 (91,800), 290 sh (29,300), 331 (24,800), 371 sh (33,300), 417 (91,800), 491 sh (720), 535 (800), 791 sh (150), 866 (235).

Ni(^{CN}Ph,^{CN}Ph)$_2$ H$_2$O, 12 H$_2$O. This procedure differs slightly from the others because of the relatively low solubility of the ligand in MeOH. A few drops of benzene were added to completely dissolve a turbid mixture of 0.146 g (0.289 mmol) H(^{CN}Ph,^{CN}Ph) and 0.0343 g (0.144 mmol) $NiCl_2 \cdot 6H_2O$ in 25 mL EtOH. The resulting solution was then heated at reflux and 0.29 mmol $(NEt_4)(OH)$ (0.20 mL of a 1.47 *M* solution in MeOH) was added by syringe. After heating the resulting orange suspension at reflux 6h, the insoluble product was collected by filtration, was washed with Et_2O (2 x 5 mL) and was dried under vacuum overnight to give 0.144 g (88%) of **12** H_2O as an orange brown solid. Mp, >350^{o}C. Anal. Calcd. (found) for $C_{64}H_{42}N_{14}NiO$: C, 71.06 (71.34); H, 3.91 (4.01); N, 18.13 (18.46). μ_{eff} (solid, 295 K) = 2.8 μ_B. IR (KBr) ν_{CN} 2222 cm^{-1}. λ_{max}, nm (ε, M^{-1}cm^{-1}): 257 (89,100), 313 sh (16,700), 398 (47,000), 454 (110,000), 543 sh (2,100), 793 sh (280), 866 (360).

Chemical Oxidation of 11.

[Ni(^{tBu}Ph,^{tBu}Ph)$_2$](BF$_4$), (11)(BF$_4$). Under an argon atmosphere, a solution of 0.0459 g (0.168 mmol) $FcBF_4$ in 20 mL CH_2Cl_2 was added via cannula transfer to a solution of 0.200 g (0.168 mmol) **11** in 20 mL CH_2Cl_2. After the resulting green solution had been stirred 1h at room temperature, solvent was removed under vacuum. The green solid was washed sequentially with one 10 mL portion of toluene, three 10 mL portions hexane, and then was dried under vacuum for 2 h to leave 0.150 g (70%) of **(11)(BF$_4$)** as a green solid. Mp, >350^{o}C. Anal. Calcd. (found) for $C_{76}H_{76}N_{10}NiBF_4$: C, 71.59 (71.77); H, 6.00 (6.05); N, 10.98 (10.79). μ_{eff} (solid, 295 K) = 2.5 μ_B. UV-Vis (CH_2Cl_2) λ_{max}, nm (ε, M^{-1}, cm^{-1}), 254 (96,300), 350sh (34,600), 404 (55,200), 602 (5,900), 725sh (5,800), 854 (16,200).

Discussion of Ligand Syntheses. The twelve pyrazolyl-containing pincer-type ligands described here and elsewhere[S2,S4,S8] were prepared by one (or more) of four main methods, as summarized in Schemes S1-S4. In the first method (Scheme S1), bromination of a diarylamine

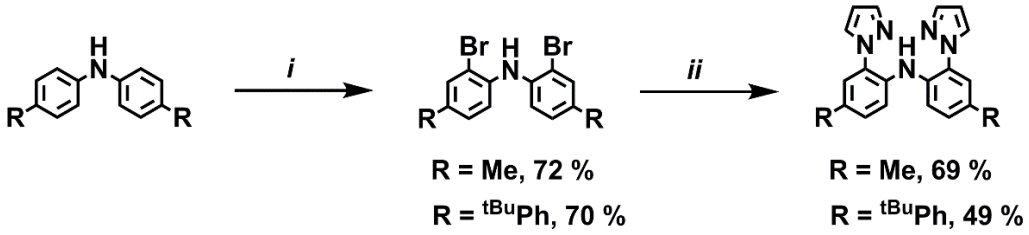

Scheme S1. Synthesis of H(Me,Me) and H(^{tBu}Ph,^{tBu}Ph) by sequential bromination and amination reactions. Key: i) 2 eq. Br_2, 1:1 (v/v) CH_2Cl_2:MeOH, 0°C, 1 h; ii) 3.5 eq. pyrazole, 3.5 equiv. K_2CO_3, 10 mol% CuI, 40 mol% DMED, xylenes, reflux 36 h.

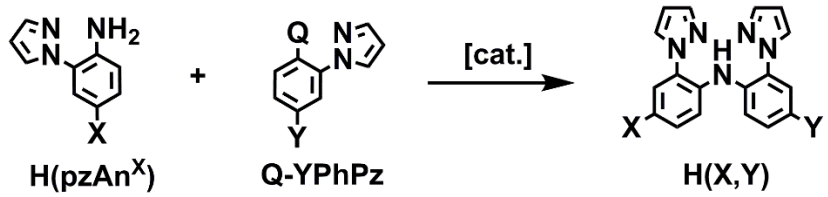

entry	X =	Q =	Y =	[cat.]	Product	Yield (%)
1	Me	Br	H	*a*	H(Me,H)	73
2	H	Br	H	*a*	H(H,H)	68
3	CO_2Et	I	Me	*b*	H(Me,CO_2Et)	73
4	Me	Br	CF_3	*a*	H(Me,CF_3)	83
5	CN	I	Me	*b*	H(Me,CN)	51
6	CF_3	Br	CF_3	*a*	H(CF_3,CF_3)	90
7	CN	Br	CN	*a*	H(CN,CN)	50

a) CuI, Cs_2CO_3, dioxane, reflux, 15h;
b) $Pd(OAc)_2$, BINAP, Cs_2CO_3, toluene, reflux 3-4 d

Scheme S2. Convergent synthetic route to H(X,Y) ligands.

followed by CuI-catalyzed coupling of pyrazole was used to produce H(Me,Me) or H(^{tBu}Ph,^{tBu}Ph). This route is not suitable for diphenylamine (in attempts to give H(H,H)) or

related unsymmetrical diarylamines with an H-atom at the para- aryl position because bromination first occurs at the *para*-aryl position. Instead, a second versatile synthetic approach can be used whereby the arms of the pincer ligand are attached via an amination reaction between a 2-halo-5-Y-aryl-*1H*-pyrazole and a 2-(pyrazolyl)-4-X-aniline, exemplified by the seven derivatives in Scheme S2. It is noted that the reactions in Scheme S2 are optimized routes. The asymmetric derivatives H(X,Y) can be prepared by using the opposite combination of reagents (interchanging X and Y of the pyrazolyl-containing reagents in Scheme S2) but the yields were found to be lower. As shown in Scheme S3, two ligands with bromide groups at the

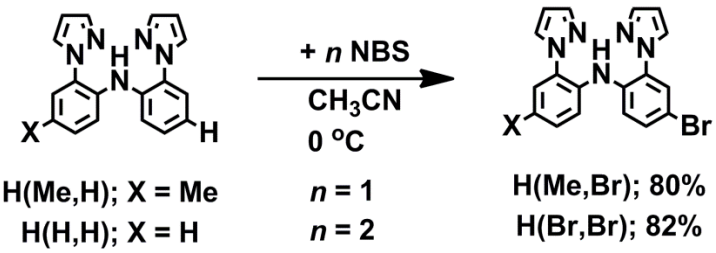

Scheme S3. Preparation of H(Me,Br) and H(Br,Br) by bromination reactions.

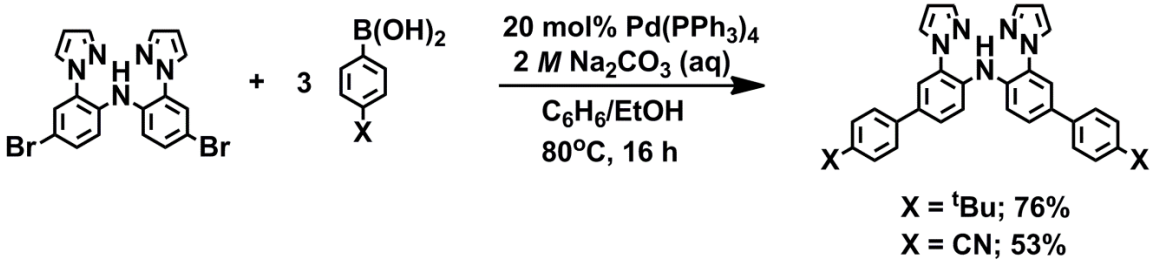

Scheme S4. Preparation of H(^{tBu}Ph,^{tBu}Ph) and H(^{CN}Ph,^{CN}Ph) by Suzuki reactions.

para-aryl position of the diarylamido backbone, H(Br,Br) and H(Me,Br), were easily accessed by bromination reactions between *N*-bromosuccinimide and either H(H,H) or H(Me,H) in CH_3CN. The use of other solvents for the bromination reactions was also successful but generally resulted in lower yields than when using CH_3CN. Finally, the derivative H(Br,Br) was

amenable to Suzuki coupling reactions to give H(^{tBu}Ph,^{tBu}Ph) or H(^{CN}Ph,^{CN}Ph) in modest to good yields, as per Scheme S4.

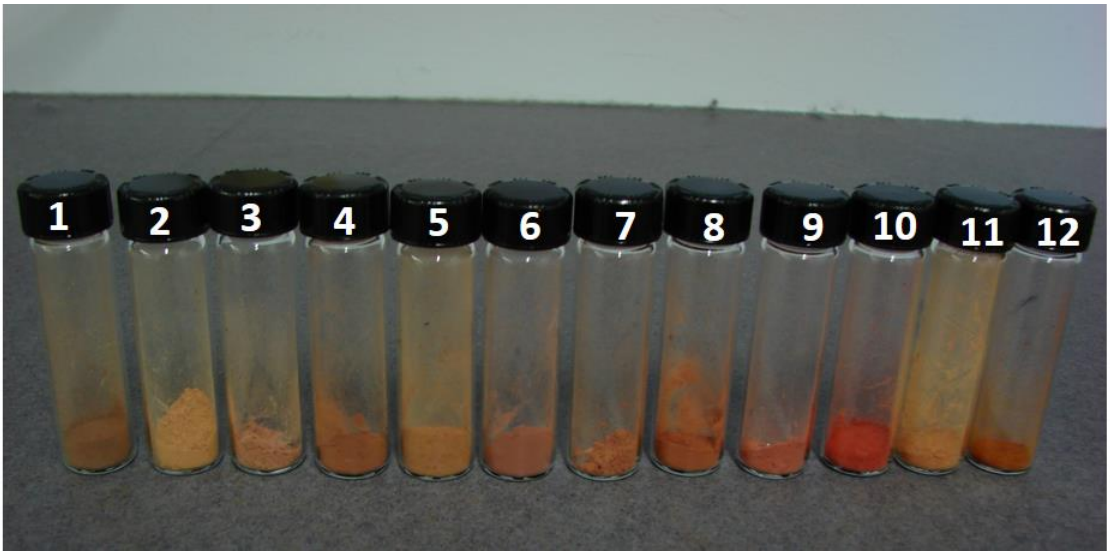

Figure S1. Photograph of compounds **1-12** as powders at room temperature.

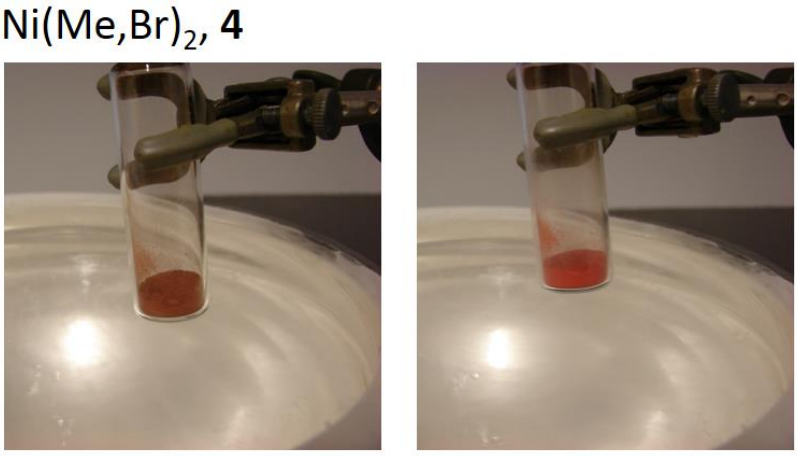

Figure S2. Photographs of compound **4** before and after cooling to 77 K showing thermochromic behavior.

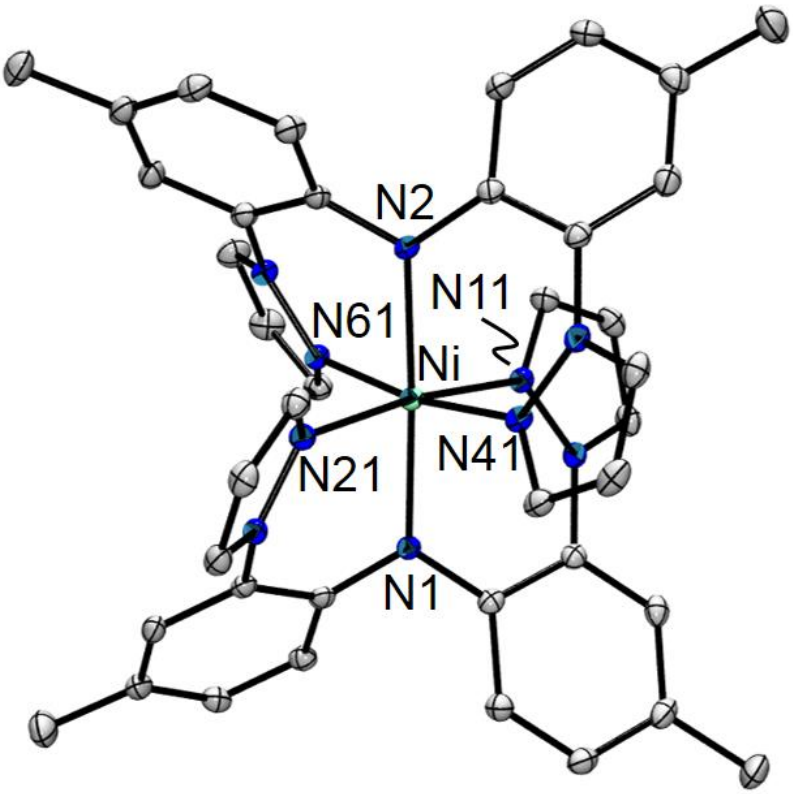

Figure S3. Molecular structure of **1** with hydrogen atoms removed for clarity. Selected bond distances (Å): Ni1-N1 2.0520(12), Ni1-N2 2.0377(12), Ni1-N11 2.0829(13), Ni1-N21 2.0880(13), Ni1-N41 2.1007(13), Ni1-N61 2.0886(13). Selected bond angles (deg.): N1-Ni1-N11 86.56(5), N1-Ni1-N21 87.56(5), N1-Ni1-N41 95.92(5), N1-Ni1-N61 91.90(5), N2-Ni1-N1 177.09(5), N2-Ni1-N11 95.73(5), N2-Ni1-N21 90.28(5), N2-Ni1-N41 85.97(5), N2-Ni1-N61 86.36(5), N11-Ni1-N21 172.93(5), N11-Ni1-N41 87.94(5), N11-Ni1-N61 88.99(5), N21-Ni1-N41 88.77(5), N21-Ni1-N61 95.12(5), N61-Ni1-N41 171.41(5).

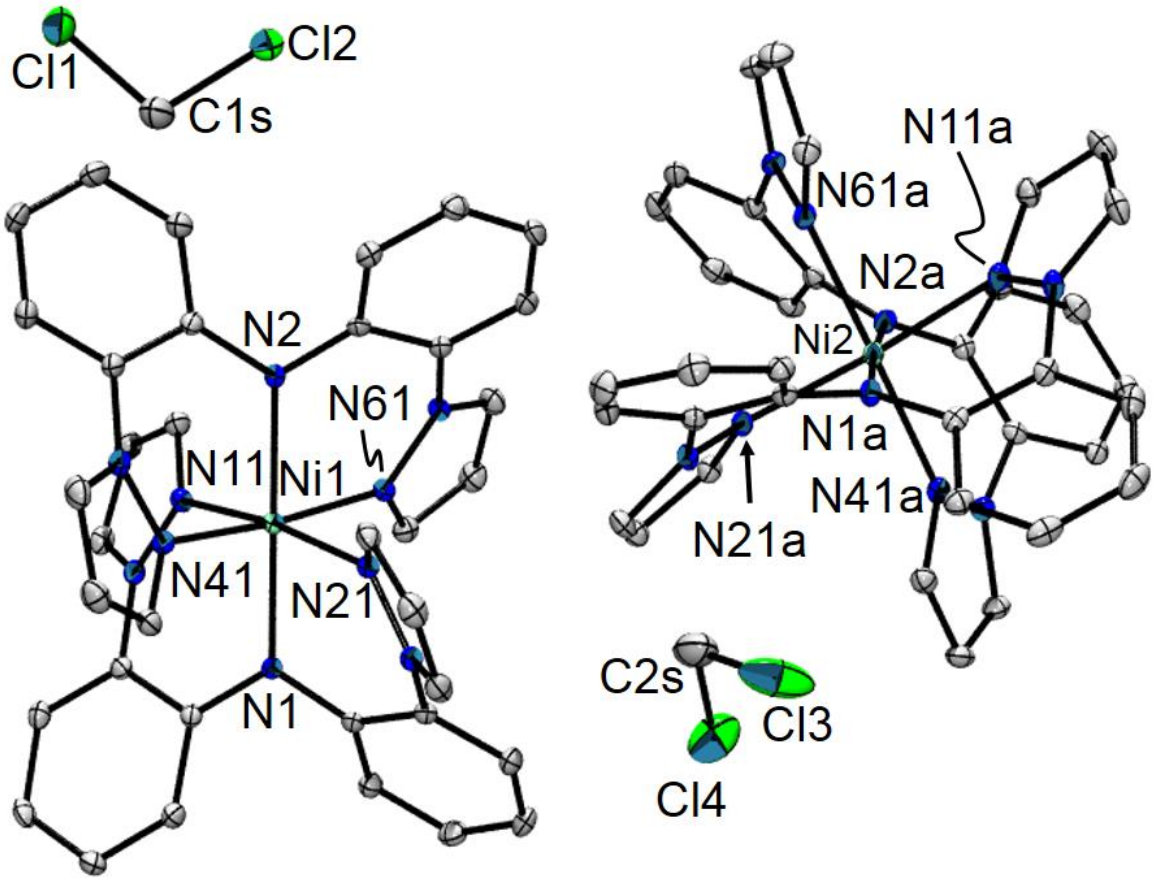

Figure S4. Molecular structure of crystallographically-independent units in **3**·CH_2Cl_2 with hydrogen atoms removed for clarity. Selected bond distances (Å): Ni1-N1 2.0307(15), Ni1-N2 2.0364(16), Ni1-N11 2.0870(16), Ni1-N21 2.1249(16), Ni1-N41 2.1061(16), Ni1-N61 2.0902(16), Ni2-N1A 2.0427(16), Ni2-N2A 2.0497(16), Ni2-N11A 2.0791(16), Ni2-N21A 2.0933(16), Ni2-N41A 2.0878(16), Ni2-N61A 2.0868(16). Selected bond angles (deg.): N1-Ni1-N2 179.95(8), N1-Ni1-N11 86.74(6), N1-Ni1-N21 86.35(6), N1-Ni1-N41 92.70(6), N1-Ni1-N61 93.40(6), N2-Ni1-N11 93.26(6), N2-Ni1-N21 93.65(6), N2-Ni1-N41 87.24(6), N2-Ni1-N61 86.66(6), N1A-Ni2-N2A 175.90(6), N1A-Ni2-N11A 87.53(6), N1A-Ni2-N21A 89.09(6), N1A-Ni2-N41A 89.05(6), N1A-Ni2-N61A 94.84(6), N2A-Ni2-N11A 90.41(6), N2A-Ni2-N21A 93.23(6), N2A-Ni2-N41A 87.61(6), N2A-Ni2-N61A 88.57(6), N11A-Ni2-N21A 174.51(6), N11A-Ni2-N41A 95.14(6), N11A-Ni2-N61A 86.59(6), N41A-Ni2-N21A 89.12(6), N61A-Ni2-N21A 89.39(6), N61A-Ni2-N41A 175.82(6).

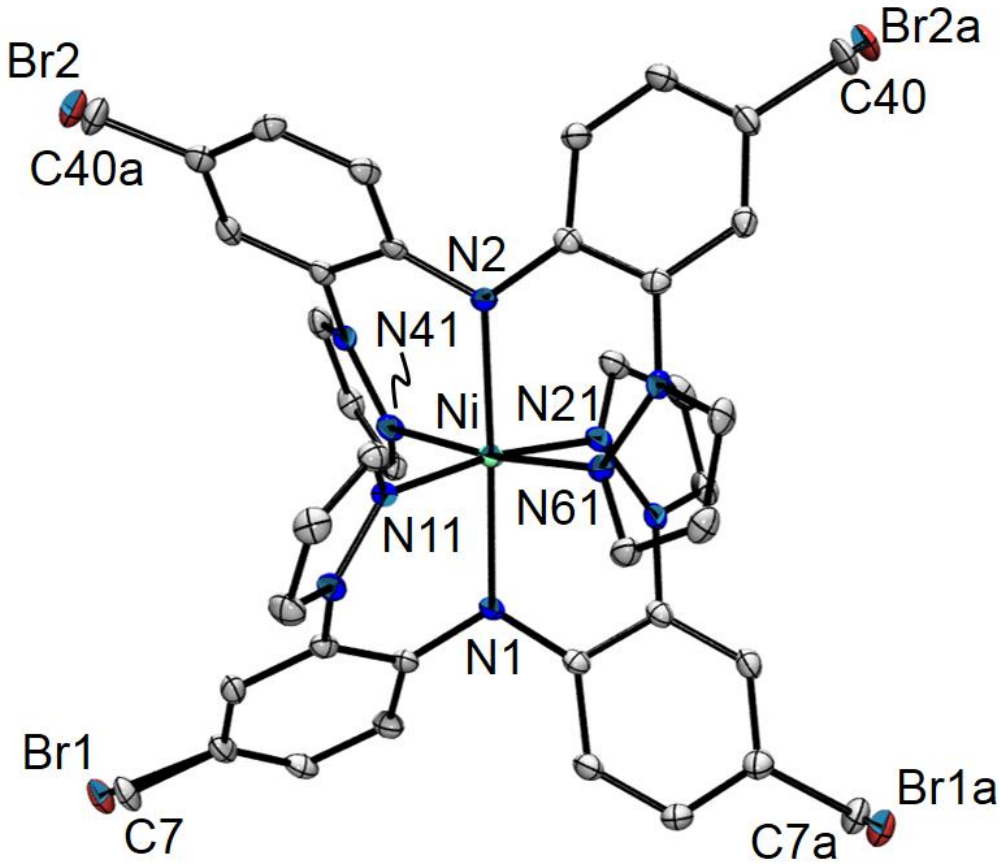

Figure S5. Molecular structure of **4** with both disorder components shown but with hydrogen atoms removed for clarity. Selected bond distances (Å): Ni1-N1 2.037(3), Ni1-N2 2.050(3), Ni1-N11 2.088(3), Ni1-N21 2.101(3), Ni1-N41 2.087(3), Ni1-N61 2.077(3). Selected bond angles (deg.): N1-Ni1-N2 177.86(11), N1-Ni1-N11 86.96(11), N1-Ni1-N21 86.23(11), N1-Ni1-N41 90.48(11), N1-Ni1-N61 95.05(11), N2-Ni1-N11 91.82(11), N2-Ni1-N21 95.09(11), N2-Ni1-N41 87.87(11), N2-Ni1-N61 86.67(11), N11-Ni1-N21 172.40(11), N41-Ni1-N11 94.54(11), N41-Ni1-N21 88.87(11), N61-Ni1-N11 88.68(11), N61-Ni1-N21 88.58(11), N61-Ni1-N41 173.75(11).

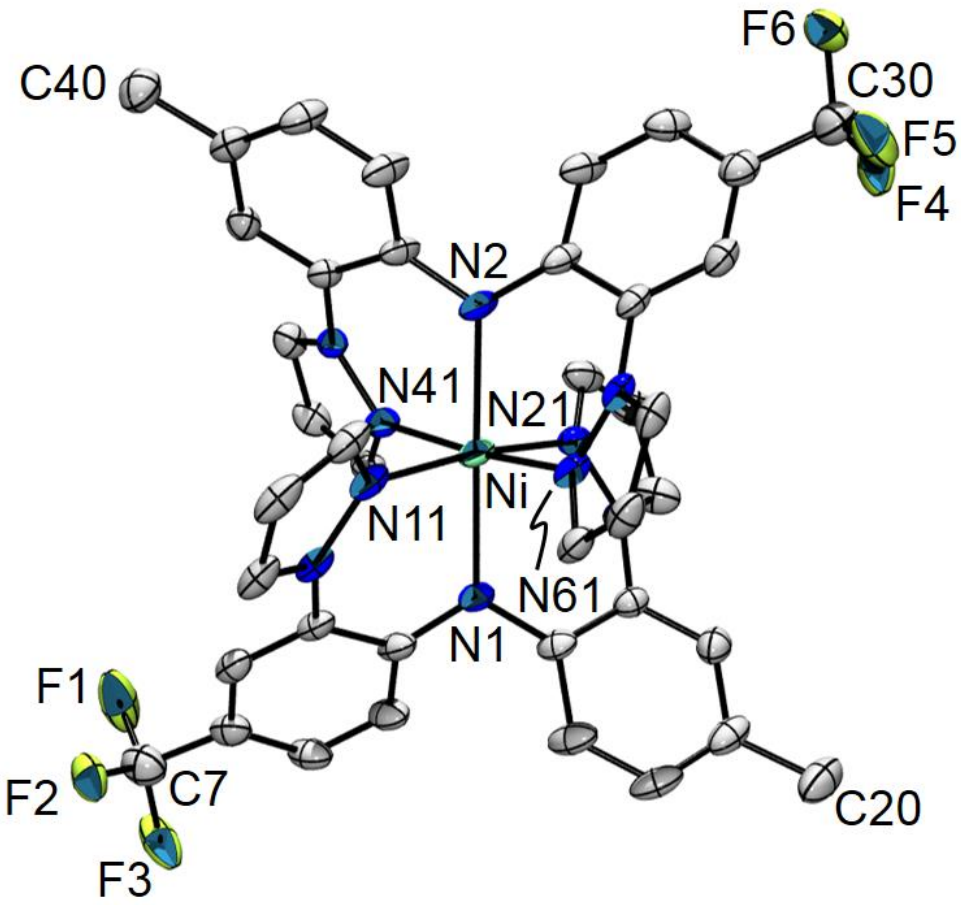

Figure S6. Molecular structure of one disorder component of **6** with hydrogen atoms removed for clarity. Selected bond distances (Å): Ni1-N11 2.093(2), Ni1-N21 2.086(2), Ni1-N1 2.0464(18), Ni1-N61 2.0849(19), Ni1-N41 2.0736(19), Ni1-N2 2.0534(18). Selected bond angles (deg.): N21-Ni1-N11 172.96(7), N1-Ni1-N11 86.38(8), N1-Ni1-N21 86.80(7), N1-Ni1-N61 91.57(8), N1-Ni1-N41 93.92(8), N1-Ni1-N2 179.02(8), N61-Ni1-N11 88.31(8), N61-Ni1-N21 93.63(8), N41-Ni1-N11 89.66(8), N41-Ni1-N21 89.06(8), N41-Ni1-N61 174.02(7), N2-Ni1-N11 94.37(8), N2-Ni1-N21 92.46(8), N2-Ni1-N61 87.84(7), N2-Ni1-N41 86.71(7).

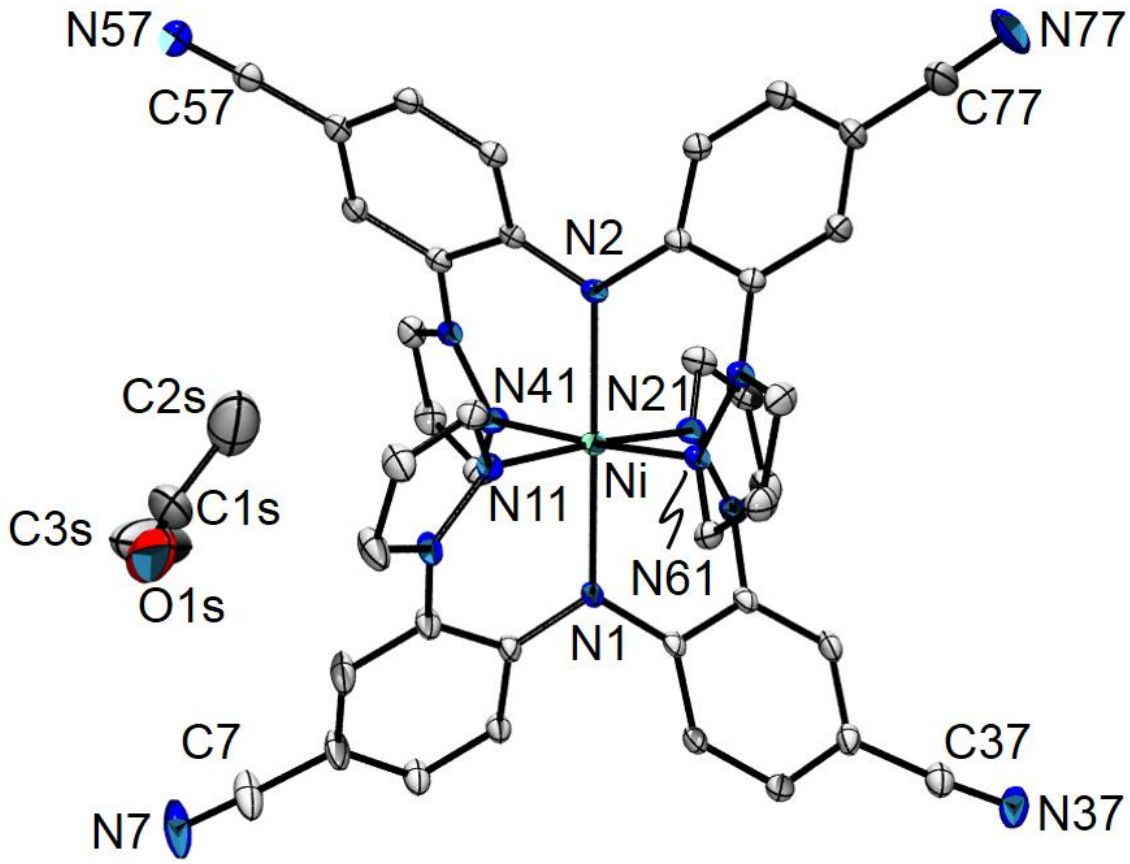

Figure S7. Structure of **10**·acetone with hydrogen atoms removed for clarity. Selected bond distances (Å): Ni1-N1 2.0481(17), Ni1-N2 2.0489(18), Ni1-N11 2.064(2), Ni1-N21 2.075(2), Ni1-N41 2.0789(19), Ni1-N61 2.0858(19). Selected bond angles (deg.): N1-Ni1-N2 179.33(8), N1-Ni1-N11 87.17(7), N1-Ni1-N21 88.84(7), N1-Ni1-N41 92.15(7), N1-Ni1-N61 91.47(7), N2-Ni1-N11 92.21(7), N2-Ni1-N21 91.79(7), N2-Ni1-N41 88.09(7), N2-Ni1-N61 88.28(7), N11-Ni1-N21 175.79(7), N11-Ni1-N41 91.27(8), N11-Ni1-N61 87.74(7), N21-Ni1-N41 87.54(8), N21-Ni1-N61 93.70(8), N41-Ni1-N61 176.20(7).

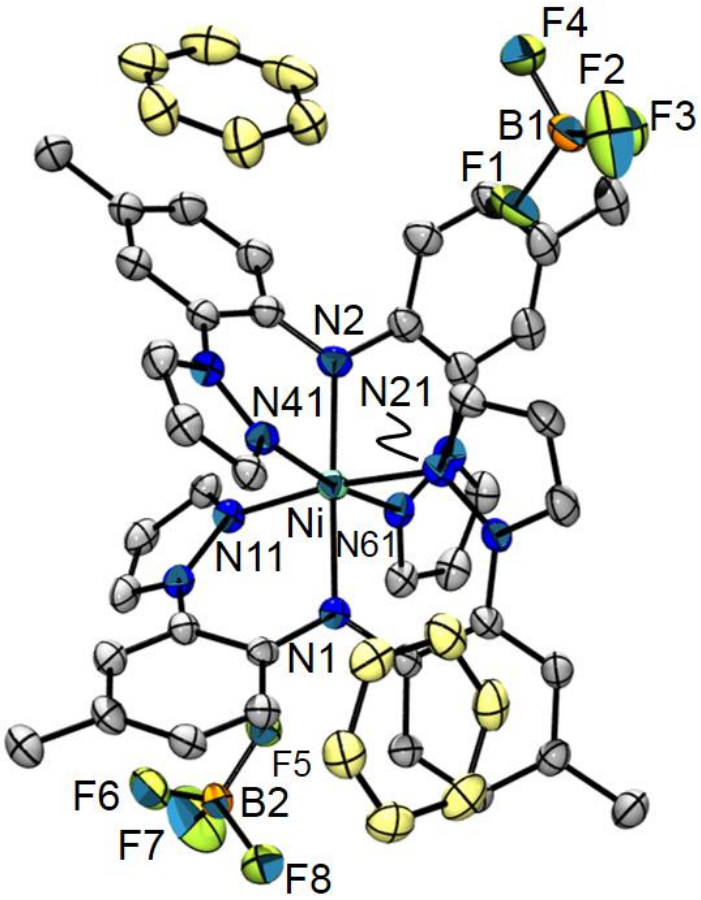

Figure S8. Structure of (**1**)$(BF_4)_2 \cdot 2C_6H_6$ with benzene solvent molecules colored goldenrod and with hydrogen atoms removed for clarity. Selected bond distances (Å): Ni1-N1 2.048(3), Ni1-N2 2.020(3), Ni1-N11 2.067(3), Ni1-N21 2.052(3), Ni1-N41 2.076(3), Ni1-N61 2.073(3). Selected bond angles (deg.): N1-Ni1-N11 86.69(12), N1-Ni1-N21 85.65(12), N1-Ni1-N41 95.57(12), N1-Ni1-N61 93.50(13), N2-Ni1-N1 178.25(15), N2-Ni1-N11 94.61(13), N2-Ni1-N21 93.07(13), N2-Ni1-N41 85.61(13), N2-Ni1-N61 85.33(14), N11-Ni1-N41 90.55(12), N11-Ni1-N61 89.66(12), N21-Ni1-N11 172.31(12), N21-Ni1-N41 89.53(13), N21-Ni1-N61 91.47(12), N61-Ni1-N41 170.93(12).

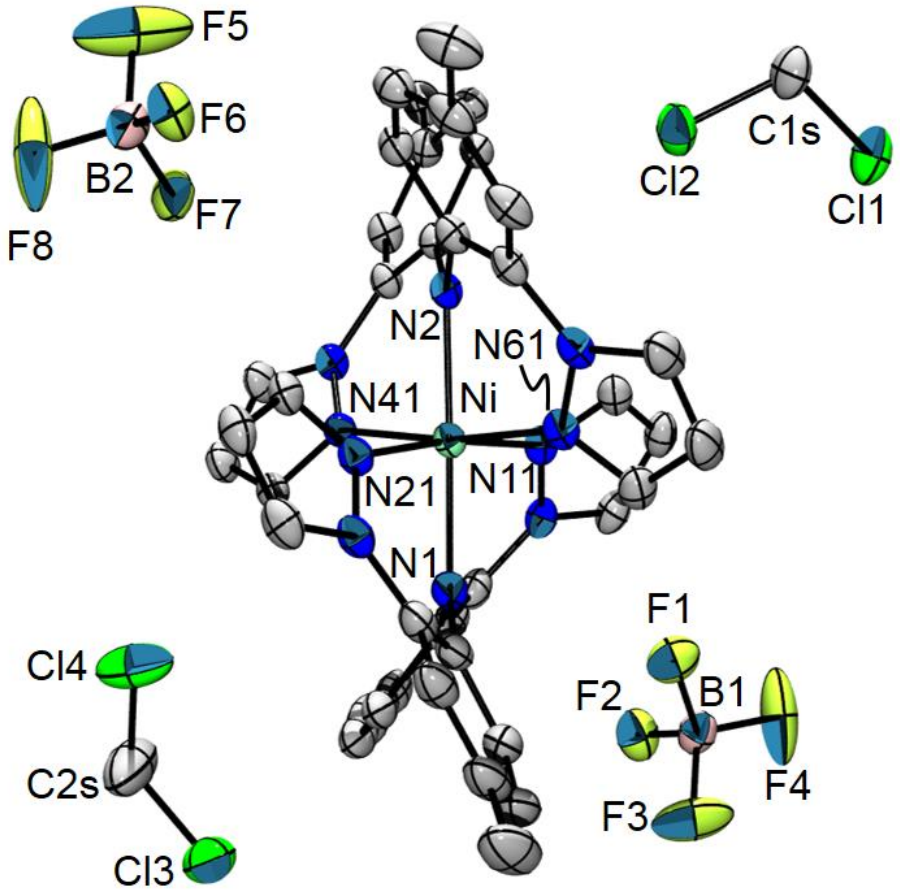

Figure S9. Structure of (**1**)$(BF_4)_2 \cdot 2CH_2Cl_2$ with hydrogen atoms removed for clarity. Selected bond distances (Å): Ni1-N1 2.042(3), Ni1-N2 2.033(3), Ni1-N11 2.074(3), Ni1-N21 2.066(3), Ni1-N41 2.057(3), Ni1-N61 2.053(3). Selected bond angles (deg.): N1-Ni1-N11 86.40(11), N1-Ni1-N21 85.79(11), N1-Ni1-N41 92.68(10), N1-Ni1-N61 95.14(11), N2-Ni1-N1 177.56(11), N2-Ni1-N11 92.83(10), N2-Ni1-N21 95.03(10), N2-Ni1-N41 85.05(10), N2-Ni1-N61 87.15(10), N21-Ni1-N11 172.05(10), N41-Ni1-N11 93.08(10), N41-Ni1-N21 88.77(10), N61-Ni1-N11 88.80(11), N61-Ni1-N21 90.43(11), N61-Ni1-N41 172.06(11).

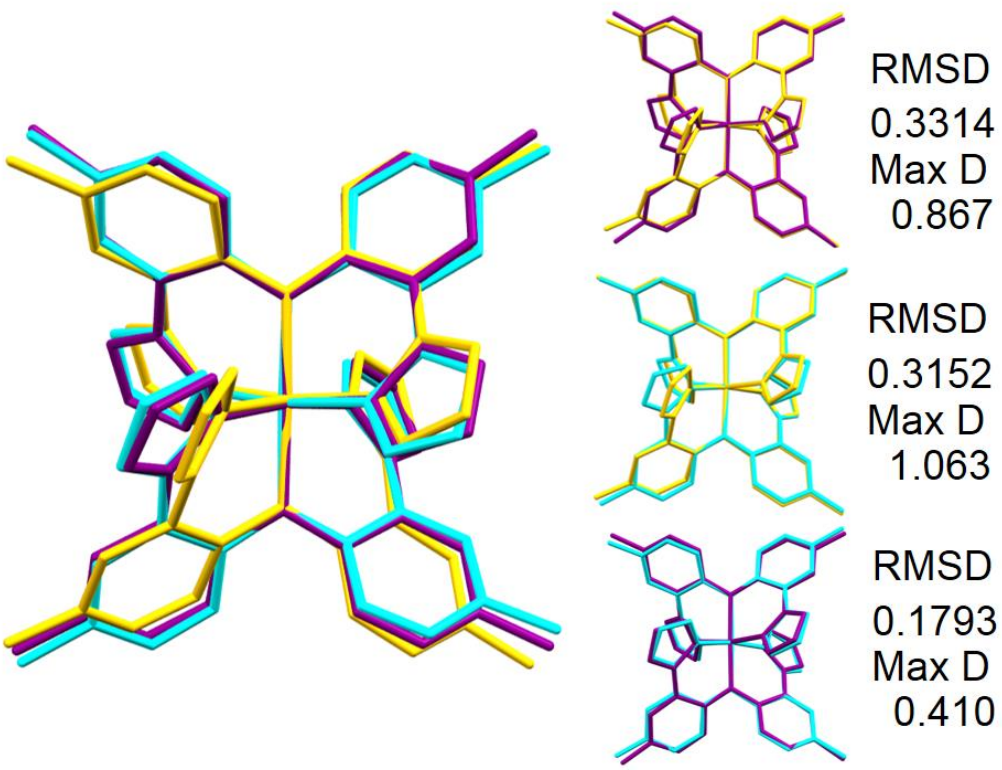

Figure S10. Overlays of nickel complexes in **1** (orange), (**1**)$(BF_4)_2 \cdot 2C_6H_6$ (cyan), and (**1**)$(BF_4)_2 \cdot 2CH_2Cl_2$ (violet).

Table S1. Intraligand bond labeling scheme and summary of important average bond distances in Å (std dev.) and angles in degrees (std dev.) in **1** and (**1**)$(BF_4)_2$.

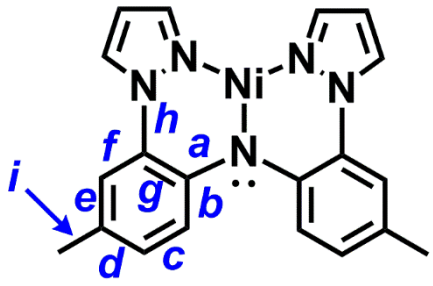

	1	(**1**)$(BF_4)_2 \cdot 2C_6H_6$	(**1**)$(BF_4)_2 \cdot 2CH_2Cl_2$	Avg. (**1**)$(BF_4)_2$	**1** – avg $(\mathbf{1})^{2+}$
Ni-N_{Ar}	2.045(7)	2.038(5)	2.034(9)	2.036(12)	+0.009
Ni-N_{pz}	2.090(8)	2.063(10)	2.067(10)	2.065(10)	+0.025
Ni-N_{all}	2.075	2.054	2.056	2.055	+0.020
Bond					
A	1.382(6)	1.383(4)	1.378(11)	1.381(8)	+0.001
B	1.416(5)	1.412(2)	1.415(5)	1.413(4)	+0.002
C	1.376(1)	1.379(5)	1.367(5)	1.373(8)	+0.003
D	1.396(2)	1.391(2)	1.394(17)	1.392(11)	+0.004
E	1.388(2)	1.390(7)	1.390(3)	1.390(5)	-0.002
F	1.393(3)	1.396(5)	1.385(7)	1.391(8)	+0.002
G	1.413(3)	1.422(4)	1.420(9)	1.421(7)	-0.008
H	1.432(6)	1.414(3)	1.423(8)	1.419(8)	+0.013
I	1.508(5)	1.510(7)	1.506(8)	1.508(8)	+0.000
Pz-Ar (°)[a]	37(6)	30(7)	27(9)	28(8)	+9

[a]dihedral angle between mean planes of pyrazolyl ring and the aryl group to which it is bound.

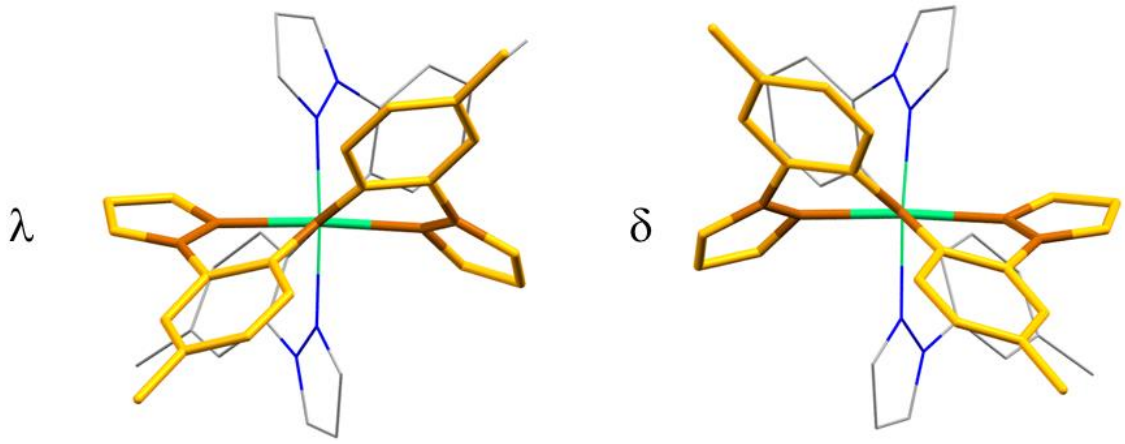

Figure S11. Isomers of Ni(Me,Me)$_2$.

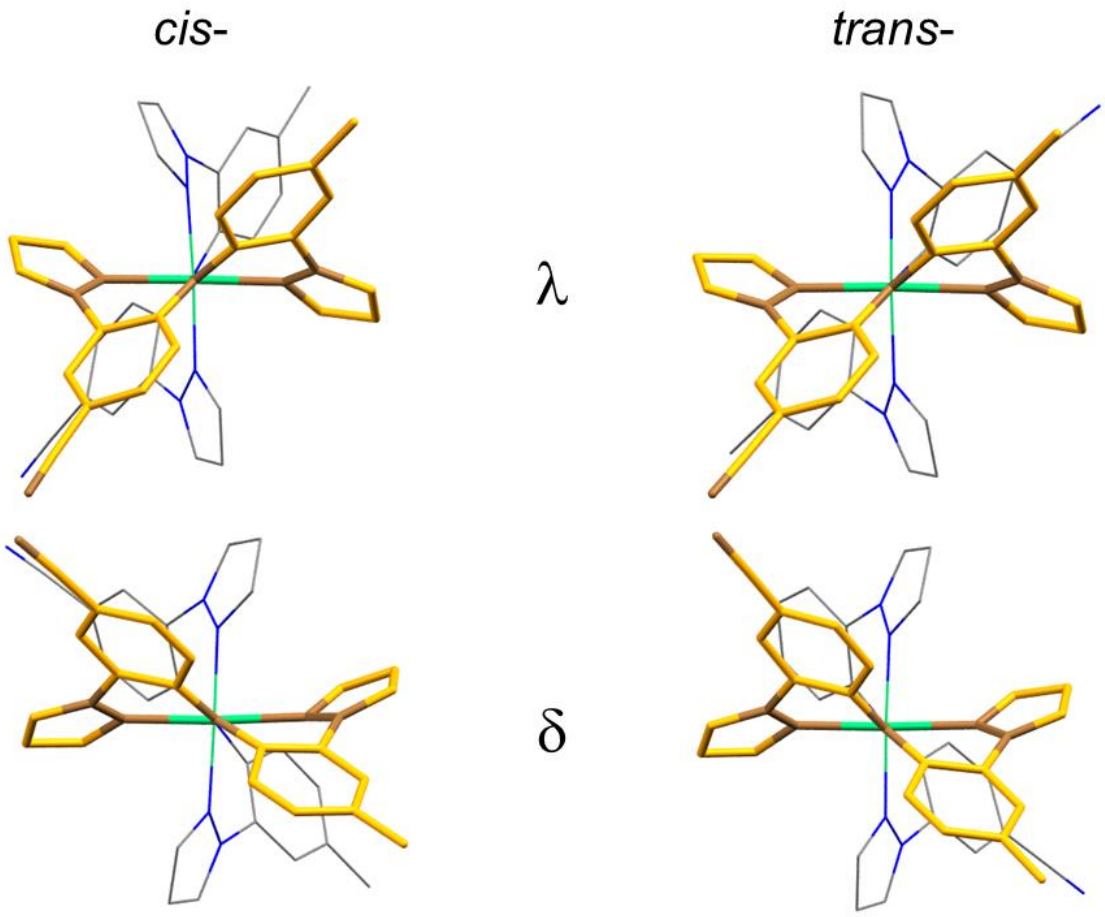

Figure S12. Isomers of Ni(Me,CN)$_2$. Cis- and trans- refer to the relative disposition of cyano-groups with respect to the central N_{Ar}-Ni-N_{Ar} bonds.

Further discussion of Electronic Spectra. A comparison of data in Table 5 reveals that changes to the *para*- aryl substituents have little impact on the ligand field strength in the twelve $Ni(X,Y)_2$ complexes as all have nearly the same value for 10Dq of 11,480(60) cm^{-1} found from

Table S2. Ligand Field and nephelauxetic parameters for $Ni(X,Y)_2$ complexes.

	$\bar{\upsilon}$, cm^{-1} (ε, $M^{-1}cm^{-1}$)					
Compound	$^3A_{2g}\rightarrow{}^3T_{2g}$	$^3A_{2g}\rightarrow{}^3T_{1g}$	$^3A_{2g}\rightarrow{}^3T_{1g}(^3P)$[a]	Δ_o/B[a]	B (cm^{-1})[b]	β (cm^{-1})[c]
$Ni(Me,Me)_2$, **1**	11,470	18,400 (180)	29,800	12.6	913	0.84
$Ni(Me,H)_2$, **2**[d]	11,520	18,480 (180)	30,130	12.3	937	0.87
$Ni(H,H)_2$, **3**[e]	11,510	18,595(170)	30,700	11.7	985	0.91
$Ni(Me,Br)_2$, **4**	11,490	18,550 (210)	30,560	12.0	976	0.90
$Ni(Me,CO_2Et)_2$, **5**[d]	11,640	18,900 (430)[e]	31,530	11.3	1034	0.96
$Ni(Me,CF_3)_2$, **6**	11,500	18,700 (170)	31,260	11.2	1030	0.95
$Ni(Br,Br)_2$, **7**	11,480	18,670 (250)	31,210	11.2	1029	0.95
$Ni(Me,CN)_2$, **8**	11,590	18,800 (380)[e]	31,280	11.4	1020	0.94
$Ni(CF_3,CF_3)_2$, **9**	11,640	18,900 (210)	31,530	11.3	1034	0.96
$Ni(CN,CN)_2$, **10**[d]	11,600	*na*	---	*na*	---	---
$Ni(^{tBu}Ph,^{tBu}Ph)_2$, **11**	11,520	*na*	---	*na*	---	---
$Ni(^{CN}Ph,^{CN}Ph)_2$, **12**[ed]	11,650	*na*	---	*na*	---	---

[a] Estimated from Tanabe Sugano diagram with C/B = 4.71. [b] estimated from $15B = E(^3A_{2g} \rightarrow {}^3T_{1g}(^3F)) + E(^3A_{2g} \rightarrow {}^3T_{1g}(^3P)) - 30Dq$.(S9) [c] $\beta = B/(B_{ion} = 1082\ cm^{-1})$. [c] from deconvolution of spectra [d] as the solvate shown in Scheme 1. [e] from the average of split bands. *na*= not available, masked by intense ligand-based transitions.

the energy of the lowest energy *d-d* ($^3A_{2g} \rightarrow {}^3T_{2g}$) transition. For the current series of complexes that have extended pi-systems (**5**, **8**, and **10**-**12**), the ligand-centered transitions extend further into the green (λ_{max} ~500 nm) than the other complexes and tend to obfuscate or completely mask the second-lowest energy spin-allowed *d-d* transition ($^3A_{2g}\rightarrow{}^3T_{1g}(^3F)$). For all complexes, the highest energy spin-allowed *d-d* transition ($^3A_{2g}\rightarrow{}^3T_{1g}(^3P)$) is hidden by the higher intensity bands for charge transfer and other ligand- based transitions. Thus, for those complexes **1**-**9** where the two lower energy spin-allowed *d-d* transition bands are observed or can clearly be extracted by deconvolution of spectra, the nephelexautic parameter β (Table S2) is calculated to

be in the range of 0.84 to 0.96, values higher than that reported for $[Ni(pyrazole)_6]^{2+}$ (β = 0.78)[S10] or $[Ni(Tpm)_2]^{2+}$ (β = 0.73).[S11] Among the series **1**-**9**,the values of β increase and appear to reach a limiting value of 0.96 as the electron withdrawing power of the four groups at the *para*- aryl positions of the $Ni(X,Y)_2$ complexes increases, as approximated by averaging the Hammett σ_p parameters of X and Y substituents.

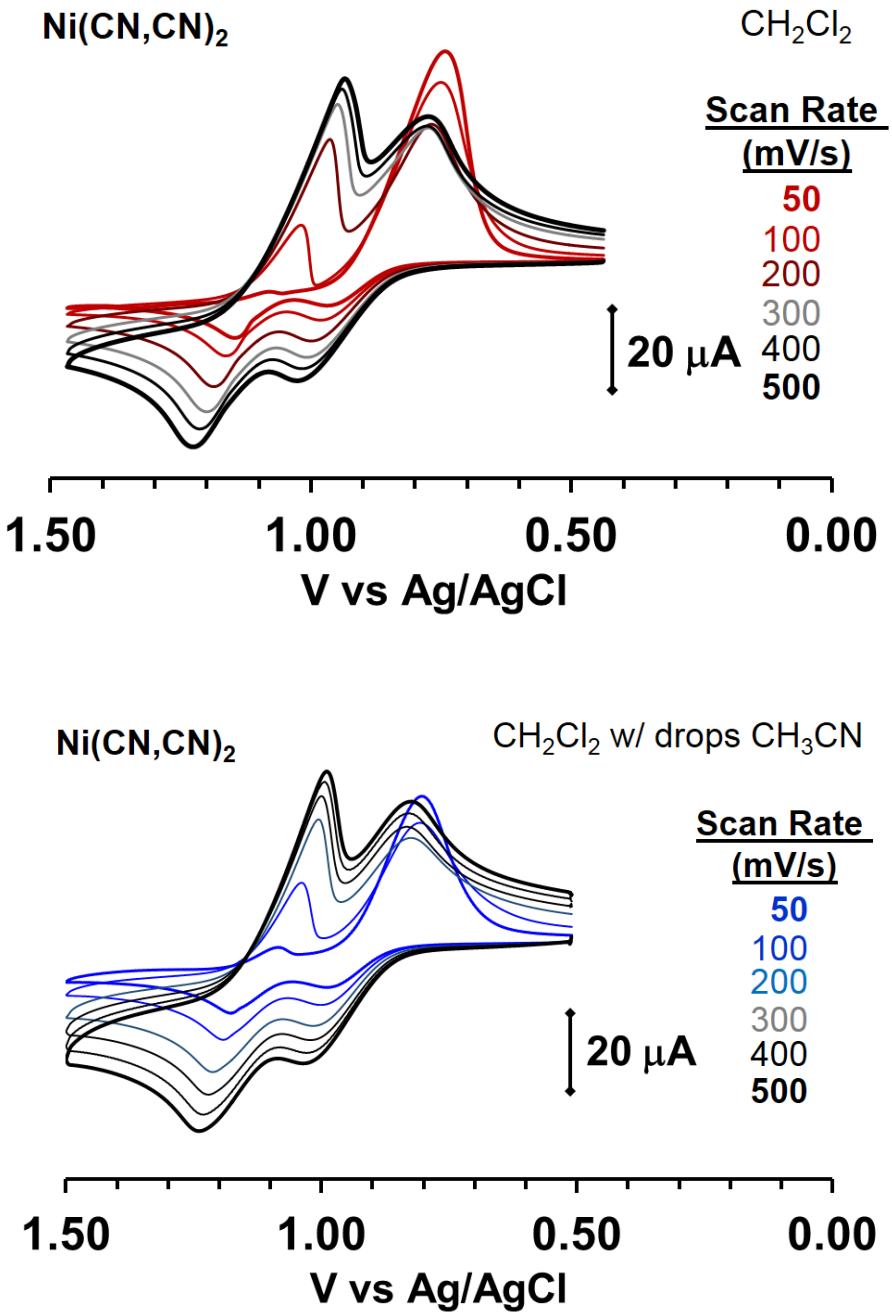

Figure S13. Cyclic voltammograms obtained for $Ni(CN,CN)_2$ in CH_2Cl_2 (top) and in CH_2Cl_2 with a few drops of CN_3CN added (bottom). In each case, NBu_4PF_6 is the supporting electrolyte.

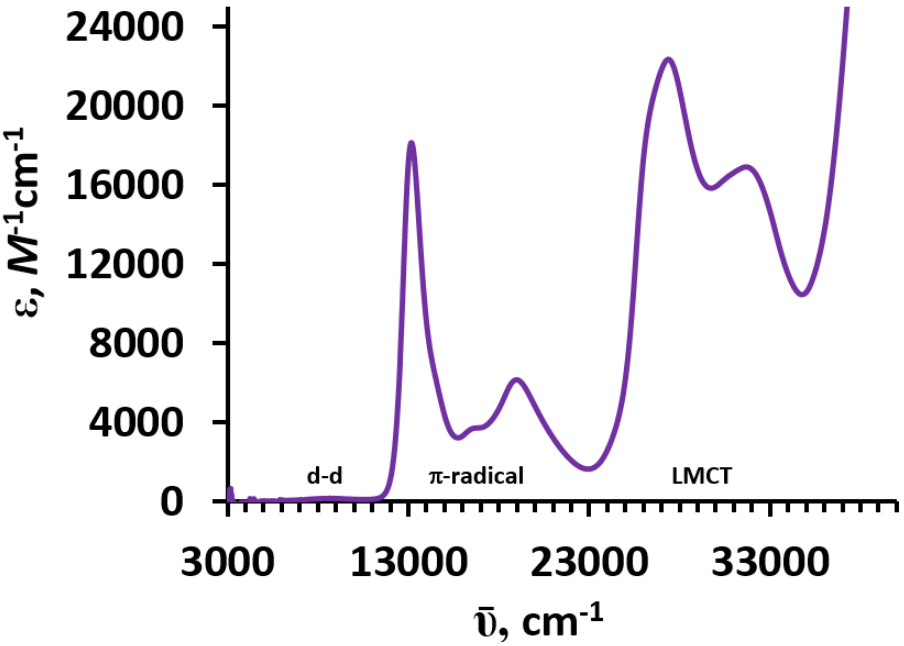

Figure S14. Visible/NIR spectrum of $[Ni(Me,Me)_2](BF_4)_2 \cdot 0.5CH_2Cl_2$ in CH_2Cl_2.

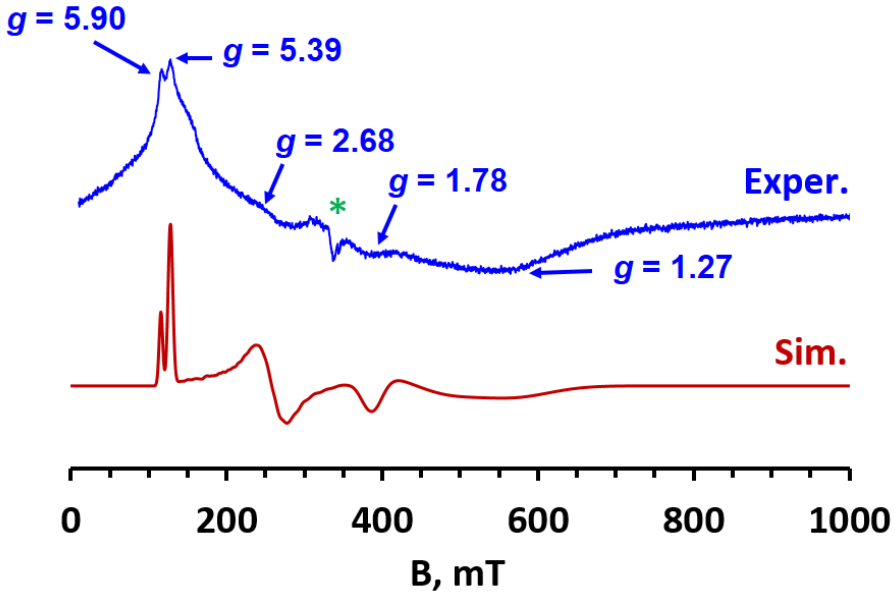

Figure S15. X-Band EPR spectrum of $[Ni(Me,Me)_2](BF_4) \cdot 0.5CH_2Cl_2$ in CH_2Cl_2 at 10 K. Instrumental parameters: Freq. = 9.632 GHz; Power = 0.2 mW, modulation 10 G.

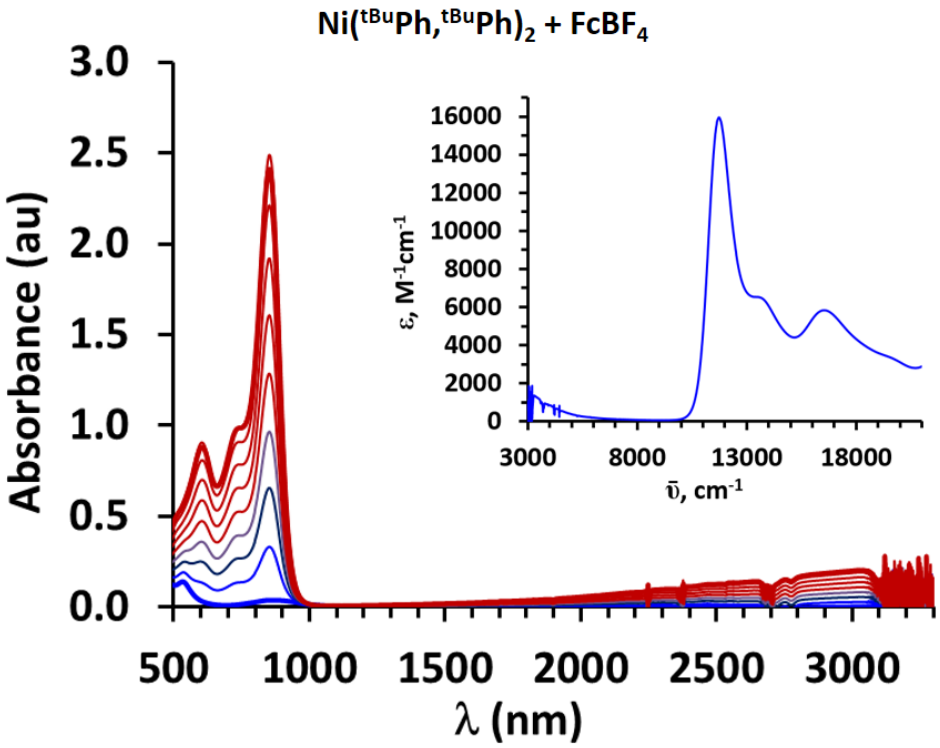

Figure S16. Vis-NIR spectra from incremental addition of $FcBF_4$ to solution of $Ni(^{tBu}Ph,^{tBu}Ph)_2$ in CH_2Cl_2. Inset: Spectra of $Ni(^{tBu}Ph,^{tBu}Ph)_2(BF_4)$ in wavenumber units.

Part 2. Computational Work.

General Considerations. DFT calculations were performed with either M06 or M06-2X meta-hybrid GGA functionals[S12] because these have been found to be useful for affording accurate solutions to a wide variety of computation problems at low computational expense.[S13,S20] Geometry optimizations used the combination of the M06 functional and the def2-SV(P) double-zeta basis set[S14] because we previously found[S8] (and find again here) that this method provides excellent agreement (within 0.2 Å) with solid state structures. Solvent (dichloromethane and acetonitrile) effects were accounted for by using the polarizable continuum model IEFPCM,[S15] as implemented in Gaussian 09.[S16] Analytical vibrational frequency calculations were carried out to verify that optimized geometries were stationary points. Time-dependent DFT methodology was used for excitation energy calculations.[S17] For instances where improved accuracy of SCF energies and thermodynamic parameters was warranted such as in broken-symmetry calculations[S18] or the determination of reduction potentials, the optimized structures were subject to single-point energy calculations using the def2-TZVP basis set[S14] that had the polarization functions on hydrogen removed (for computational time-saving reasons). The calculation of reduction potentials at the double-zeta quality def2-SV(P) level followed Truhlar's methodology[S19] and used recommendations outlined recently by Rulíšek.[S20] For estimation of reduction potentials at the triple zeta level, which would be prohibitively costly on our computational cluster, the zero-point energy and thermal corrections for each **1**, $(\mathbf{1})^{+}$, and $(\mathbf{1})^{2+}$ were taken from the calculations performed at the def2-SV(P) level and were applied to the SCF energies obtained from single point calculations at the def2-TZVP level.

Table S3. Summary of SCF energies and thermochemical data from theoretical calculations (M06/Def2-SV(P)).

	Ni(Me,Me)$_2$	**[Ni(Me,Me)$_2$]$^+$**	**[Ni(Me,Me)$_2$]$^{2+}$**
multiplicity	3	4	5
<S^2>	2.0081/2.000	3.7907/3.7508	6.0774/6.0025
E$_{SCF}$(hartree)	-3598.484935	-3598.314711	-3598.131557
E+ZPE(hartree)	-3597.797706	-3597.626693	-3597.442173
H (hartree)	-3597.753662	-3597.582026	-3597.397927
G (hartree)	-3597.873960	-3597.704346	-3597.517799

Table S4. Bond Labeling diagram and calculated (M06/Def2-SV(P)) bond distances and angles in Ni(Me,Me)$_2$, [Ni(Me,Me)$_2$]$^+$, and [Ni(Me,Me)$_2$]$^{2+}$. Average experimental values are given for comparison.

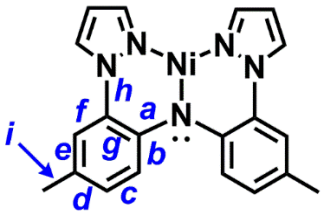

	Calculated Average (std. dev.)[a]			**Experimental**	
	Ni(Me,Me)$_2$	[Ni(Me,Me)$_2$]$^+$	[Ni(Me,Me)$_2$]$^{2+}$	**1**	Avg.
Ni-N$_{Ar}$	2.061(1)	2.044(19)	2.060(1)	2.045(7)	2.036(12)
Ni-N$_{pz}$	2.108(1)	2.082(6)	2.072(1)	2.090(8)	2.065(10)
Ni-N$_{all}$	2.092	2.070	2.068	2.075	2.055
Bond					
A	1.373	1.370	1.367	1.382(6)	1.381(8)
B	1.419	1.417	1.418	1.416(5)	1.413(4)
C	1.384	1.383	1.381	1.376(1)	1.373(8)
D	1.404	1.404	1.404	1.396(2)	1.392(11)
E	1.391	1.395	1.400	1.388(2)	1.390(5)
F	1.400	1.396	1.390	1.393(3)	1.391(8)
G	1.418	1.424	1.429	1.413(3)	1.421(7)
H	1.425	1.421	1.417	1.432(6)	1.419(8)
I	1.499	1.496	1.493	1.508(5)	1.508(8)
Pz-Ar (°)[b]	41(1)	34(3)	32(1)	37(6)	28(8)

[a]bond distances in Å; [b]dihedral angle between the mean plane of a pyrazolyl ring and that of the aryl group to which it is bound.

Figure S17. Calculated bond distances (Å) within $[Ni(Me,Me)_2]^+$. The values in black represent distances associated with an oxidized ligand whereas those in violet are typical of a non-oxidized ligand. The values in bold are C-C and C-N bonds that show greatest discrepency.

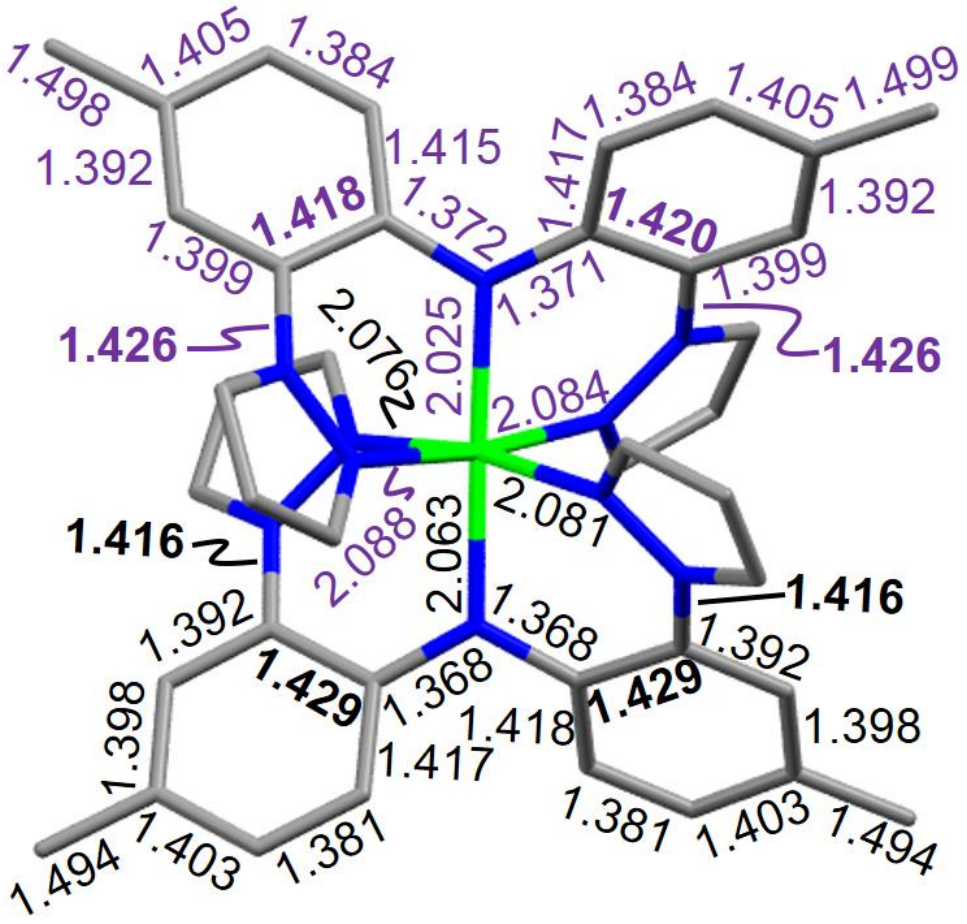

Fig. S18. β-frontier Orbitals of Ni(Me,Me)$_2$, **1** from DFT calculations (M06/Def2-SV(P)).

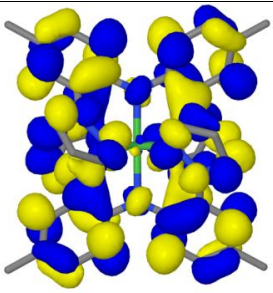

-0.027 eV

β-LUMO(+7), 194

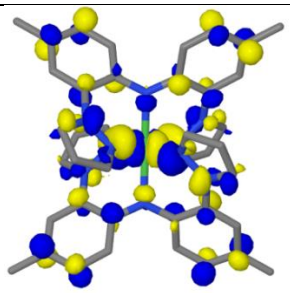

+0.517 eV

β-LUMO(+8), 195

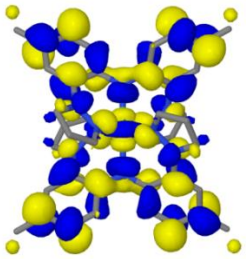

+0.707 eV

β-LUMO(+10), 197

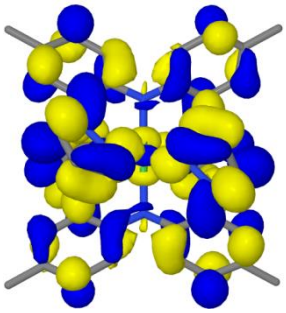

-0.571 eV

β-LUMO(+2), 189

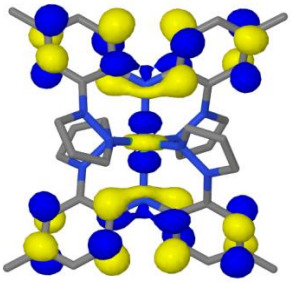

-0.299 eV

β-LUMO(+4), 191

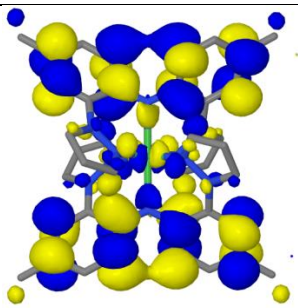

-0.245 eV

β-LUMO(+5), 192

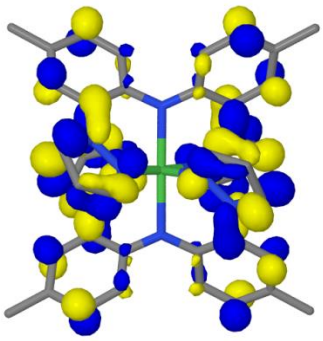

-0.898 eV

β-LUMO, 187

Fig. S18, cont'd. β-frontier Orbitals of Ni(Me,Me)$_2$, **1** from DFT calculations (M06/Def2-SV(P)).

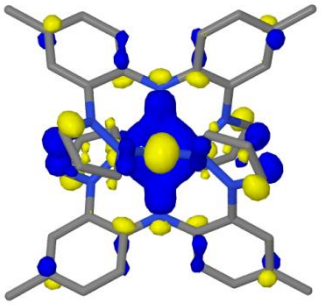	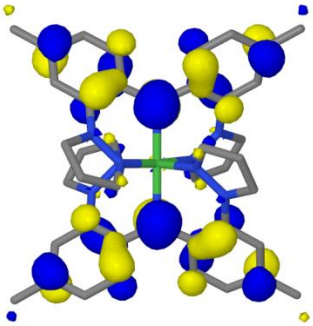	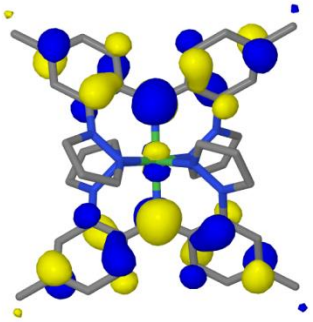
-6.912 eV	**-4.798 eV**	**-4.871 eV**
β-HOMO(-6), 180	**β-HOMO(-1), 185**	**β-HOMO, 186**

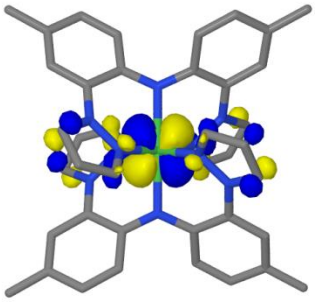	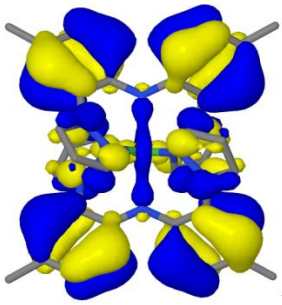	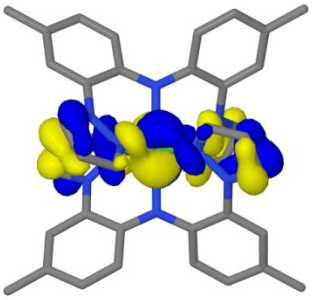
-7.265 eV	**-7.184 eV**	**-7.075 eV**
β-HOMO(-10), 176	**β-HOMO(-9), 177**	**β-HOMO(-8), 178**

	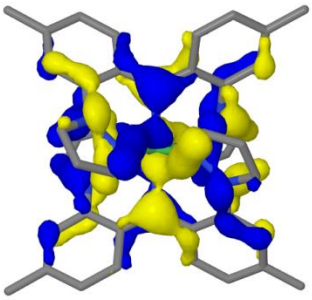	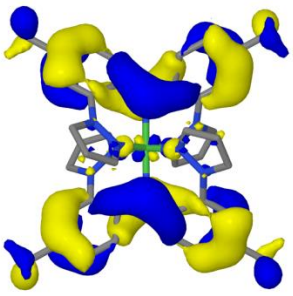
	-8.653 eV	**-8.163 eV**
	β-HOMO(-21)	**β-HOMO(-16), 170**

Fig. S19. β-frontier Orbitals of $[Ni(Me,Me)_2]^+$, $(\mathbf{1})^+$, from DFT calculations (M06/Def2-SV(P)).

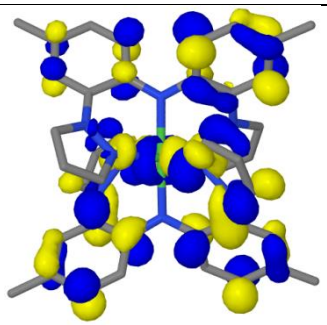

-1.116 eV

β-LUMO(+5), 191

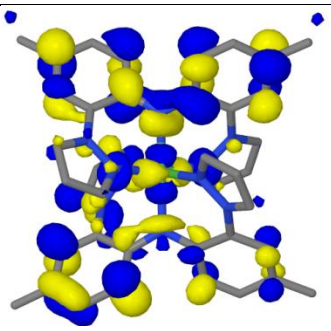

-0.843 eV

β-LUMO(+6), 192

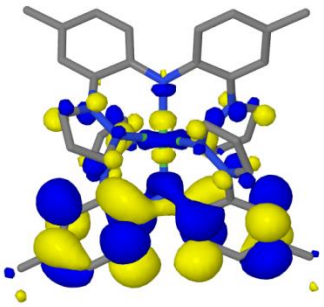

-0.354 eV

β-LUMO(+8), 194

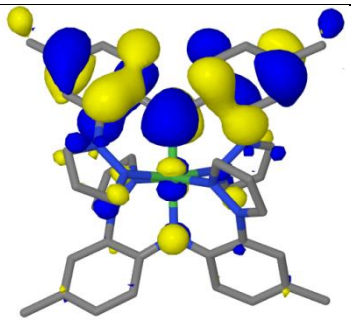

-4.272 eV

β-LUMO, 186

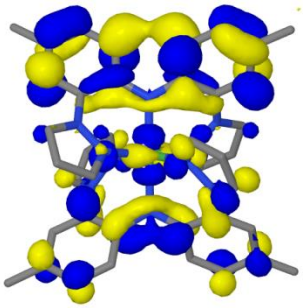

-1.415 eV

β-LUMO(+2), 188

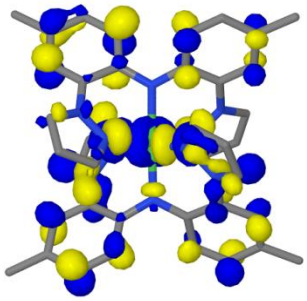

-1.170 eV

β-LUMO(+4), 190

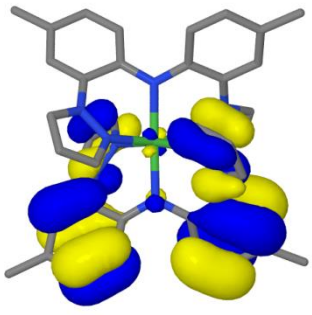

-7.211 eV

β-HOMO(-2), 183

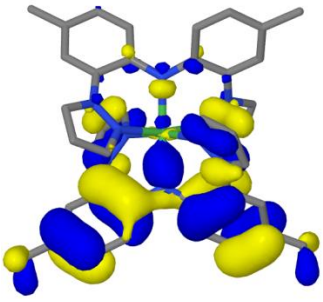

-6.748 eV

β-HOMO(-1), 184

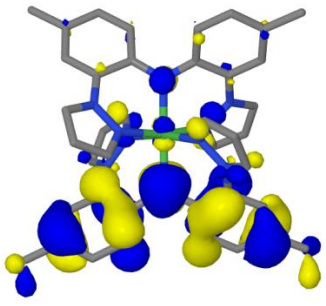

-5.252 eV

β-HOMO, 185

Fig. S19, cont'd. β-frontier Orbitals of $[Ni(Me,Me)_2]^+$, $(\mathbf{1})^+$, from DFT calculations (M06/Def2-SV(P)).

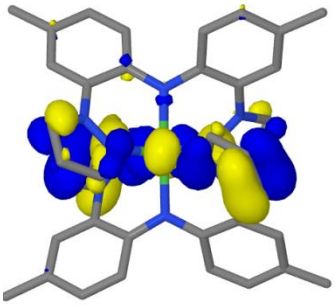	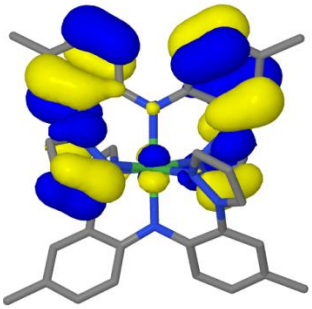	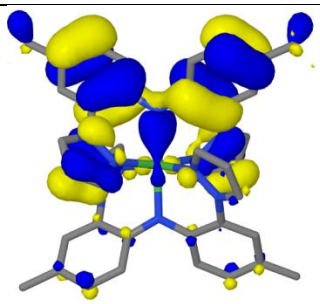
-7.701 eV	**-7.646 eV**	**-7.265 eV**
β-HOMO(-6), 179	**β-HOMO(-5), 180**	**β-HOMO(-3), 182**

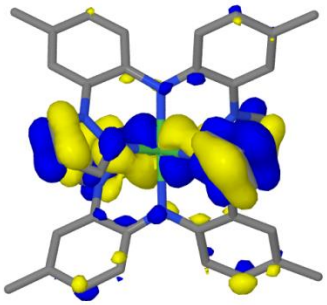	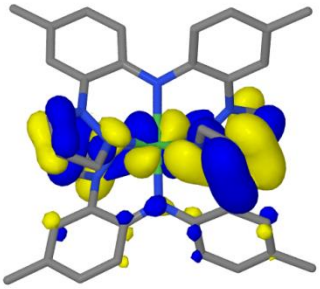	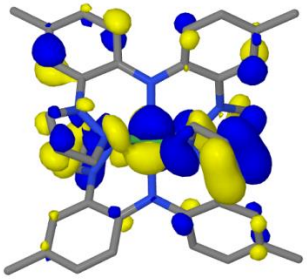
-8.327 eV	**-7.973 eV**	**-7.728 eV**
β-HOMO(-12), 173	**β-HOMO(-9), 176**	**β-HOMO(-7), 178**

	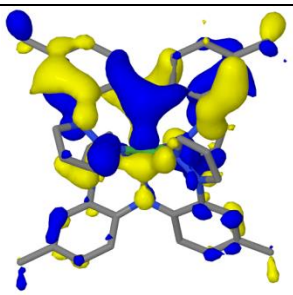	
	-9.469 eV	
	β-HOMO(-20), 165	

Fig. S20. β-frontier Orbitals of $[Ni(Me,Me)_2]^{2+}$, $(\mathbf{1})^{2+}$, from DFT calculations (M06/Def2-SV(P)).

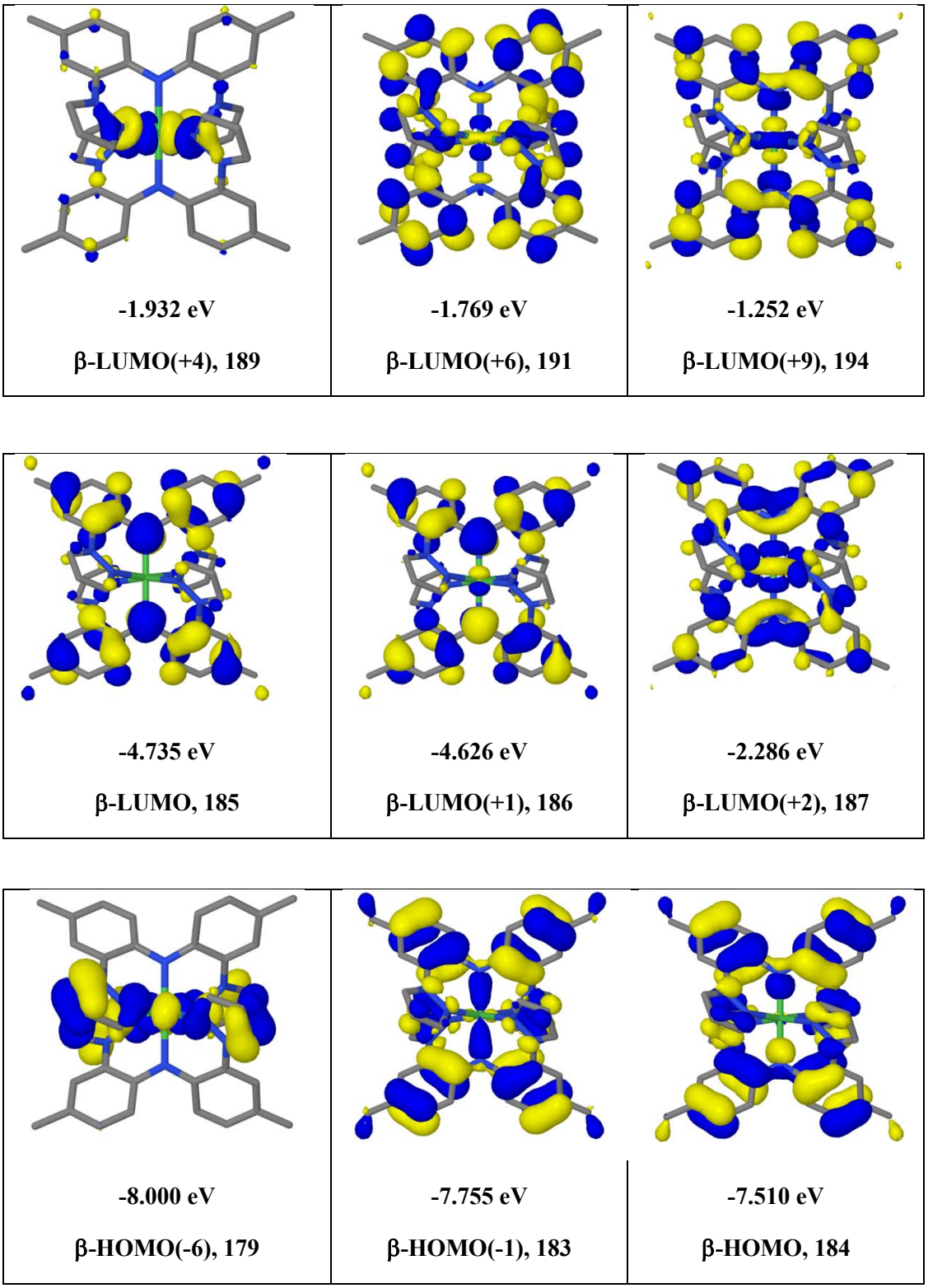

Fig. S20, Cont'd. β-frontier Orbitals of $[Ni(Me,Me)_2]^{2+}$, $(\mathbf{1})^{2+}$, from DFT calculations (M06/Def2-SV(P)).

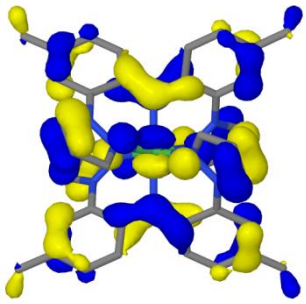	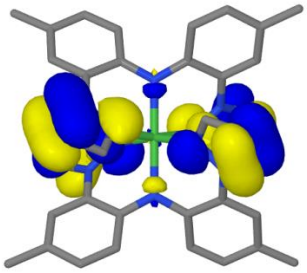	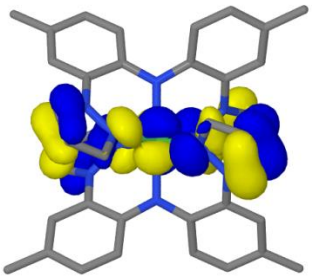
-8.925 eV	**-8.599 eV**	**-8.436 eV**
β-HOMO(-10), 175	**β-HOMO(-8), 177**	**β-HOMO(-7), 178**
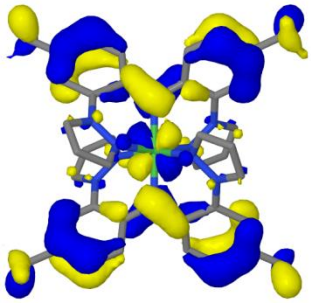	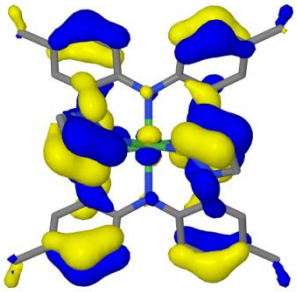	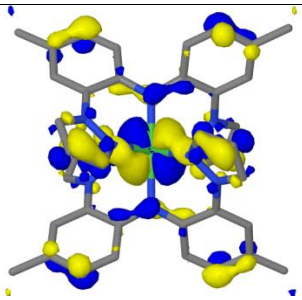
-9.470 eV	**-9.388 eV**	**-9.061 eV**
β-HOMO(-14), 171	**β-HOMO(-12), 173**	**β-HOMO(-11), 174**
	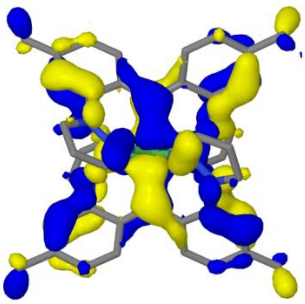	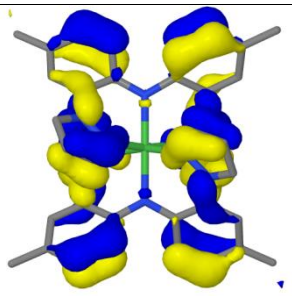
	-10.123 eV	**-9.578 eV**
	β-HOMO(-18), 167	**β-HOMO(-15), 170**

Table S5. TDDFT/TDA Excitation Energies and Transitions of Ni(Me,Me)$_2$, **1** in CH_2Cl_2 (PCM).

Total Energy First Excited state, E(TD-HF/TD-KS) = -3598.44615144

Excited State	Excitation energy (eV)	Oscillator Strength	Origin[a]	Amplitude[a]	Transition moment			Dipole Strength
					X	Y	Z	(AU)
1	1.0554	0.0000	180 β →192 β	-0.72715	-0.0044	0.0032	0.0150	0.0003
		$<S^2>$=2.005	180 β →187 β	-0.46781				
			170 β →192 β	-0.25366				
			165 β →192 β	-0.25362				
2	1.1765	0.0001	186 β →192 β	0.34359	0.0411	0.0437	0.0095	0.0037
		$<S^2>$=2.009	186 β →187 β	0.25747				
			177 β →192 β	0.50379				
			177 β →187 β	0.32145				
			176 β →189 β	-0.32030				
3	1.2012	0.0009	186 β →189 β	0.32798	-0.0845	-0.1563	-0.0139	0.0318
		$<S^2>$=2.009	177 β →197 β	-0.27048				
			177 β →189 β	0.42708				
			176 β →192 β	-0.39998				
			176 β →187 β	-0.25701				
4	1.8986	0.0011	186 β →189 β	0.26625	-0.0847	-0.1249	-0.0170	0.0231
		$<S^2>$=2.013	177 β →189 β	0.27254				
			176 β →192 β	0.60064				
			176 β →187 β	0.39568				
5	1.9092	0.0002	177 β →192 β	0.25757	-0.0082	0.0628	-0.0082	0.0041
		$<S^2>$=2.011	176 β →197 β	0.34510				
			176 β →194 β	0.30219				
			176 β →189 β	0.57709				

[a]Key: 186 β = β-HOMO, 177 β = β-HOMO(-9), 187 β = β-LUMO, 192 β = β-LUMO (+5), etc. [b] only those transitions with |amplitude| greater than 0.25 are given.

Table S6. TDDFT/TDA Excitation Energies and Transitions of $[Ni(Me,Me)_2]^+$, $(\mathbf{1})^+$ in CH_2Cl_2 (PCM).

Total Energy First Excited state, E(TD-HF/TD-KS) = -3598.30408717

Excited State	Excitation energy (eV)	Oscillator Strength	Origin[a]	Amplitude[a]	Transition moment			Dipole Strength
					X	Y	Z	(AU)
1	0.2891	0.0197	185 β →186 β	0.99892	-0.4989	0.1284	1.5847	2.7767
		$<S^2>$=3.800						
2	1.2408	0.0000	179 β →191 β	0.47571	0.0019	0.0045	-0.0081	0.0001
		$<S^2>$=3.787	179 β →190 β	0.54695				
			169 β →190 β	0.26044				
3	1.4100	0.0001	178 β →192 β	0.32884	-0.0400	-0.0100	-0.0093	0.0018
		$<S^2>$=3.791	178 β →188 β	0.33447				
			176 β →192 β	0.25522				
			176 β →188 β	0.25021				
4	1.4708	0.0000	178 β →191 β	0.34286	0.0255	0.0106	0.0219	0.0012
		$<S^2>$=3.790	178 β →190 β	0.40776				
			173 β →190 β	-0.27144				
5	1.6065	0.0420	184 β →186 β	0.81019	0.5836	0.8336	0.1744	1.0659
		$<S^2>$=3.805	182 β →186 β	-0.55071				
6	1.8778	0.0741	184 β →186 β	0.55892	-0.6462	-1.0830	-0.1454	1.6116
		$<S^2>$=3.805	182 β →186 β	0.79844				
7	2.0250	0.0000	173 β →192 β	0.31035	0.0030	0.0013	-0.0084	0.0001
		$<S^2>$=3.803	173 β →188 β	0.30746				
8	2.1294	0.0002	178 β →190 β	-0.27528	-0.0288	-0.0574	-0.0040	0.0041
		$<S^2>$=3.794	176 β →191 β	-0.32555				
			176 β →190 β	-0.39615				
			173 β →191 β	-0.25134				
			173 β →190 β	-0.30664				
9	2.1773	0.0135	179 β →186 β	0.92785	-0.3108	-0.3908	-0.0540	0.2523
		$<S^2>$=3.801						
10	2.2037	0.0119	183 β →186 β	-0.47210	0.1118	-0.0318	-0.4544	0.2200
		$<S^2>$=3.819	180 β →186 β	0.84175				

[a]Key: 185 β = β-HOMO, 179 β = β-HOMO(-6), 186 β = β-LUMO, 190 β = β-LUMO (+4), etc. [b] only those transitions with |amplitude| greater than 0.25 are given.

Table S7. TDDFT/TDA Excitation Energies and Transitions of $[Ni(Me,Me)_2]^{2+}$, $(\mathbf{1})^{2+}$ in CH_2Cl_2 (PCM).

Total Energy First Excited state, E(TD-HF/TD-KS) = -3598.08354430

Excited State	Excitation energy (eV)	Oscillator Strength	Origin[a]	Amplitude[a]	Transition moment			Dipole Strength
					X	Y	Z	(AU)
1	1.3065	0.0000	178 β →189 β	-0.72348	-0.0003	-0.0024	0.0002	0.0000
		$<S^2>$=6.074	171 β →189 β	-0.42407				
			167 β →189 β	-0.41522				
2	1.4996	0.0001	177 β →194 β	-0.29135	0.0137	0.0378	0.0012	0.0016
		$<S^2>$=6.075	177 β →187 β	0.49323				
			174 β →187 β	0.31016				
			173 β →189 β	-0.42660				
3	1.5313	0.0001	177 β →189 β	0.43314	0.0331	-0.0145	0.0127	0.0015
		$<S^2>$=6.075	175 β →187 β	-0.26196				
			174 β →189 β	0.27286				
			173 β →194 β	0.30600				
			173 β →187 β	-0.49562				
4	1.6802	0.0031	184 β →186 β	0.79410	0.0658	0.2655	-0.0007	0.0748
		$<S^2>$=6.088	183 β →185 β	0.56170				
5	1.6958	0.2455	184 β →185 β	0.85426	-1.2000	-2.1022	-0.2233	5.9092
		$<S^2>$=6.090	183 β →186 β	0.46133				
6	2.1699	0.0003	182 β →185 β	0.79416	0.0436	0.0029	-0.0557	0.0050
		$<S^2>$=6.111	181 β →186 β	0.55903				
7	2.1888	0.0215	182 β →186 β	0.67616	0.1639	-0.0771	-0.6061	0.4001
		$<S^2>$=6.112	181 β →185 β	0.69666				
8	2.1919	0.0000	177 β →189 β	0.35591	0.0265	0.0046	-0.0084	0.0008
		$<S^2>$=6.075	174 β →189 β	-0.27333				
			173 β →189 β	0.31916				
			173 β →187 β	0.51948				
9	2.1975	0.0002	177 β →189 β	0.25976	-0.0237	-0.0346	0.0371	0.0031
		$<S^2>$=6.075	177 β →187 β	0.31563				
			175 β →189 β	0.29708				
			173 β →189 β	0.55846				
			170 β →189 β	0.27052				
10	2.2044	0.0000	178 β →194 β	-0.36167	-0.0026	-0.0004	-0.0072	0.0001
		$<S^2>$=6.075	178 β →191 β	0.25881				
			178 β →187 β	0.63765				
			171 β →187 β	0.34520				
			167 β →187 β	0.32889				

[a]Key: 184 β = β-HOMO, 177 β = β-HOMO(-7), 185 β = β-LUMO, 189 β = β-LUMO (+4), etc. [b] only those transitions with |amplitude| greater than 0.25 are given.

Table S8. Summary of results from high-spin and broken-symmetry calculations of $(\mathbf{1})^{n+}$ by different methods.

Ni(Me,Me)$_2$, **1**		M06/Def2-SV(P)	M06-2X/Def2-SV(P)	M06-2X/Def2-TZVP
S = 1	E_{SCF}(a.u.)	-3598.484935	-3599.186298	-3601.704281
[L(↓↑)-Ni(↑↑)-L(↑)]	$<S^2>$	2.0000	2.0000	2.0000

[Ni(Me,Me)$_2$]$^+$, $(\mathbf{1})^+$		M06/Def2-SV(P)	M06-2X/Def2-SV(P)	M06-2X/Def2-TZVP
S = ½	E_{SCF}(a.u.)	-3598.283206	-3598.998370	-3601.515304
[L(↓↑)-Ni(↑↑)-L(↓)]	$<S^2>$	0.7602	0.8286	0.7500
S = $^3/_2$	E_{SCF}(a.u.)	-3598.314711	-3599.000998	-3601.517916
[L(↓↑)-Ni(↑↑)-L(↑)]	$<S^2>$	3.7508	3.7504	3.7504

[Ni(Me,Me)$_2$]$^{2+}$, $(\mathbf{1})^{2+}$		M06/Def2-SV(P)	M06-2X/Def2-SV(P)	M06-2X/Def2-TZVP
S = 0	E_{SCF}(a.u.)	-3598.125971	-3598.772199	-3601.288097
[L(↓)-Ni(↑↑)-L(↓)]	$<S^2>$	2.0634/4.664	1.9760/4.4552	0.0000
S = 1	E_{SCF}(a.u.)	-3598.128374	-3598.795150	-3601.289931
[L(↓)-Ni(↑↑)-L(↑)]	$<S^2>$	2.1517	2.1087	2.0018
S = 2	E_{SCF}(a.u.)	-3598.131557	-3598.818192	-3601.330271
[L(↑)-Ni(↑↑)-L(↑)]	$<S^2>$	6.0025	6.0015	6.0015

Table S9. Cartesian Coordinates of Ni(Me,Me)$_2$, **1**, from M06/Def2-SV(P).

Atom	*X*	*Y*	*Z*
C	0.1148	0.0613	0.8591
C	0.8677	-0.1517	3.5177
C	0.1621	-1.2386	1.4240
C	0.4705	1.1971	1.5974
C	0.8425	1.1259	2.9358
C	0.5509	-1.2837	2.7879
H	0.4555	2.1735	1.0957
H	0.6136	-2.2704	3.2639
H	1.1711	-0.2575	4.5684
N	-0.0665	-2.3809	0.6963
C	-0.7395	-3.4249	1.2808
C	-2.3114	-5.5971	2.3556
C	-0.4451	-4.7842	1.0026
C	-1.8479	-3.2191	2.1431
C	-2.5981	-4.2578	2.6652
C	-1.2292	-5.8262	1.5121
H	-2.1199	-2.1830	2.3810
H	-3.4529	-4.0279	3.3162
H	-0.9782	-6.8567	1.2286
C	1.2096	2.3477	3.7229
H	1.2278	3.2497	3.0854
H	2.2071	2.2475	4.1926
H	0.4911	2.5366	4.5446
C	-3.1438	-6.7184	2.9002
H	-3.0975	-6.7647	4.0058
H	-2.8076	-7.6969	2.5128
H	-4.2125	-6.6025	2.6346
N	-0.3667	0.2780	-0.4645
N	0.7007	-5.1523	0.2402
N	-0.0164	-0.4967	-1.5045
N	1.0483	-4.5263	-0.8958
C	2.1014	-5.1763	-1.3778
H	2.5693	-4.8224	-2.3009
C	2.4496	-6.2535	-0.5464
H	3.2638	-6.9671	-0.6710
C	1.5289	-6.2012	0.4831
H	1.4037	-6.8174	1.3746
C	-0.5861	0.0361	-2.5800
H	-0.4521	-0.4498	-3.5509
C	-1.3191	1.1853	-2.2420
H	-1.8984	1.8338	-2.8989
C	-1.1571	1.3037	-0.8747
H	-1.5527	2.0253	-0.1587
C	3.1254	-1.2153	-2.9851
C	2.7671	-0.2457	-5.5568
C	2.0524	-1.7493	-3.7435
C	3.9531	-0.2068	-3.4925
C	3.8045	0.2967	-4.7810
C	1.9231	-1.2198	-5.0532
H	4.7422	0.1970	-2.8447
H	1.1029	-1.6018	-5.6744
H	2.6068	0.1303	-6.5767
N	1.1506	-2.6485	-3.2323
C	0.6639	-3.6473	-4.0384
C	-0.2714	-5.9082	-5.5708
C	-0.6696	-4.1217	-3.9521
C	1.4896	-4.3472	-4.9556
C	1.0419	-5.4272	-5.6962
C	-1.1035	-5.2340	-4.6828
H	2.5316	-4.0171	-5.0535
H	1.7367	-5.9349	-6.3793
H	-2.1355	-5.5813	-4.5423
C	4.6947	1.3774	-5.3161
H	5.4410	1.6950	-4.5662
H	4.1172	2.2748	-5.6122
H	5.2469	1.0466	-6.2173
C	-0.7416	-7.1017	-6.3467
H	-0.6434	-6.9458	-7.4385
H	-1.8020	-7.3287	-6.1360
H	-0.1526	-8.0075	-6.1033
N	3.4568	-1.7417	-1.7030
N	-1.6452	-3.4453	-3.1641
N	2.5348	-2.0386	-0.7728
N	-1.4030	-3.0110	-1.9163
C	-2.5437	-2.4987	-1.4682
H	-2.5759	-2.0620	-0.4658
C	-3.5558	-2.6031	-2.4367
H	-4.5919	-2.2720	-2.3687
C	-2.9372	-3.2122	-3.5122
H	-3.3075	-3.4865	-4.5011
C	3.2003	-2.4633	0.2956
H	2.6406	-2.7927	1.1756
C	4.5857	-2.4381	0.0662
H	5.3876	-2.7282	0.7448
C	4.7087	-1.9742	-1.2296
H	5.5836	-1.8045	-1.8585
Ni	0.5420	-2.5149	-1.2687

Table S10. Cartesian Coordinates of $[Ni(Me,Me)_2]^+$, $(\mathbf{1})^+$, from M06/Def2-SV(P).

Atom	*X*	*Y*	*Z*
C	0.6420	-0.0611	0.8481
C	1.3918	-0.5160	3.4784
C	0.3527	-1.3332	1.4094
C	1.3634	0.9023	1.5620
C	1.7565	0.7022	2.8818
C	0.7215	-1.4957	2.7675
H	1.6288	1.8427	1.0623
H	0.5018	-2.4597	3.2429
H	1.6750	-0.7081	4.5220
N	-0.1222	-2.3741	0.6540
C	-0.9783	-3.3135	1.1711
C	-3.0076	-5.2039	1.9308
C	-0.9071	-4.6812	0.8025
C	-2.0702	-2.9610	2.0001
C	-3.0460	-3.8701	2.3697
C	-1.9202	-5.5818	1.1482
H	-2.1493	-1.9132	2.3158
H	-3.8847	-3.5354	2.9949
H	-1.8514	-6.6169	0.7899
C	2.5287	1.7371	3.6422
H	2.7626	2.6137	3.0124
H	3.4860	1.3340	4.0254
H	1.9645	2.0996	4.5233
C	-4.0914	-6.1718	2.2969
H	-4.1524	-6.3201	3.3924
H	-3.9250	-7.1612	1.8352
H	-5.0867	-5.8122	1.9716
N	0.1376	0.3184	-0.4305
N	0.2376	-5.2103	0.1370
N	-0.0077	-0.5407	-1.4544
N	0.9129	-4.5500	-0.8211
C	1.9208	-5.3374	-1.1860
H	2.6288	-4.9960	-1.9462
C	1.9009	-6.5408	-0.4657
H	2.5946	-7.3781	-0.5335
C	0.8134	-6.4170	0.3770
H	0.4213	-7.0811	1.1481
C	-0.5531	0.1450	-2.4545
H	-0.7842	-0.3613	-3.3957
C	-0.7574	1.4832	-2.0875
H	-1.1933	2.2860	-2.6812
C	-0.3106	1.5524	-0.7820
H	-0.3125	2.3745	-0.0657
C	2.7722	-0.8679	-2.9416
C	2.2173	-0.0515	-5.5616
C	1.8865	-1.6561	-3.7399
C	3.3007	0.3144	-3.4512
C	3.0362	0.7512	-4.7531
C	1.6658	-1.2186	-5.0704
H	3.9351	0.9351	-2.8085
H	0.9712	-1.7976	-5.6894
H	1.9826	0.2691	-6.5835
N	1.1483	-2.6837	-3.2190
C	0.8173	-3.7784	-3.9694
C	0.3706	-6.2846	-5.2570
C	-0.4049	-4.4953	-3.7817
C	1.7605	-4.3433	-4.8640
C	1.5487	-5.5577	-5.4867
C	-0.5864	-5.7278	-4.4030
H	2.7151	-3.8220	-4.9971
H	2.3238	-5.9734	-6.1412
H	-1.5075	-6.2893	-4.2105
C	3.6233	2.0253	-5.2672
H	3.8012	2.7509	-4.4542
H	2.9675	2.4960	-6.0206
H	4.5991	1.8404	-5.7585
C	0.1317	-7.6037	-5.9169
H	-0.3415	-7.4668	-6.9094
H	-0.5426	-8.2427	-5.3204
H	1.0771	-8.1492	-6.0840
N	3.2178	-1.2885	-1.6650
N	-1.4991	-3.9564	-3.0615
N	2.4731	-2.0571	-0.8485
N	-1.3547	-3.0946	-2.0372
C	-2.5735	-2.7699	-1.6359
H	-2.6934	-2.0713	-0.8040
C	-3.5467	-3.4300	-2.4092
H	-4.6308	-3.3586	-2.3307
C	-2.8232	-4.1737	-3.3139
H	-3.1469	-4.8081	-4.1390
C	3.2071	-2.2952	0.2267
H	2.7961	-2.9096	1.0321
C	4.4621	-1.6667	0.1243
H	5.2846	-1.6867	0.8382
C	4.4348	-1.0373	-1.1002
H	5.1997	-0.4667	-1.6273
Ni	0.4955	-2.5538	-1.2666

Table S11. Cartesian Coordinates of $[Ni(Me,Me)_2]^{2+}$, $(\mathbf{1})^{2+}$, from M06/Def2-SV(P).

Atom	*X*	*Y*	*Z*
C	0.6827	-0.0656	0.8976
C	1.3764	-0.6095	3.5563
C	0.3576	-1.3409	1.4561
C	1.3901	0.8617	1.6543
C	1.7569	0.6143	2.9826
C	0.6953	-1.5553	2.8167
H	1.6811	1.8146	1.1990
H	0.4734	-2.5357	3.2524
H	1.6568	-0.8313	4.5926
N	-0.1000	-2.3740	0.6891
C	-0.9612	-3.3166	1.1776
C	-3.0591	-5.1248	1.8451
C	-0.9406	-4.6697	0.7203
C	-2.0280	-2.9414	2.0320
C	-3.0477	-3.8159	2.3527
C	-1.9885	-5.5260	1.0372
H	-2.0692	-1.9015	2.3748
H	-3.8767	-3.4732	2.9826
H	-1.9850	-6.5450	0.6344
C	2.5130	1.6331	3.7695
H	3.0921	2.3090	3.1169
H	3.2040	1.1565	4.4868
H	1.8201	2.2626	4.3619
C	-4.1659	-6.0709	2.1749
H	-3.9740	-6.5737	3.1434
H	-4.2719	-6.8612	1.4118
H	-5.1312	-5.5440	2.2748
N	0.2145	0.3387	-0.3777
N	0.1709	-5.2131	0.0297
N	-0.0182	-0.5244	-1.3869
N	0.9537	-4.4892	-0.7946
C	1.9118	-5.3027	-1.2187
H	2.6794	-4.9266	-1.9005
C	1.7586	-6.5866	-0.6688
H	2.3934	-7.4596	-0.8140
C	0.6412	-6.4894	0.1299
H	0.1708	-7.2172	0.7912
C	-0.5076	0.1899	-2.3915
H	-0.7837	-0.3072	-3.3252
C	-0.5970	1.5484	-2.0440
H	-0.9718	2.3734	-2.6483
C	-0.1342	1.6045	-0.7486
H	-0.0670	2.4399	-0.0517
C	2.7283	-0.8136	-2.9964
C	2.1232	-0.0534	-5.6228
C	1.8549	-1.6345	-3.7749
C	3.2215	0.3727	-3.5279
C	2.9295	0.7819	-4.8346
C	1.6065	-1.2269	-5.1094
H	3.8508	1.0177	-2.9049
H	0.9189	-1.8320	-5.7108
H	1.8707	0.2460	-6.6466
N	1.1482	-2.6688	-3.2270
C	0.8420	-3.7952	-3.9364
C	0.4665	-6.3682	-5.1032
C	-0.3500	-4.5477	-3.6937
C	1.7891	-4.3593	-4.8276
C	1.6100	-5.6064	-5.3920
C	-0.4963	-5.8125	-4.2522
H	2.7209	-3.8098	-5.0017
H	2.3857	-6.0208	-6.0461
H	-1.3923	-6.3990	-4.0197
C	3.4785	2.0617	-5.3732
H	3.6435	2.8044	-4.5734
H	2.8070	2.5015	-6.1310
H	4.4557	1.8913	-5.8668
C	0.2685	-7.7209	-5.7029
H	-0.1936	-7.6369	-6.7065
H	-0.3983	-8.3492	-5.0876
H	1.2295	-8.2479	-5.8362
N	3.2010	-1.2142	-1.7215
N	-1.4536	-4.0056	-2.9891
N	2.4871	-1.9887	-0.8804
N	-1.3280	-3.0758	-2.0215
C	-2.5577	-2.7447	-1.6511
H	-2.7031	-1.9928	-0.8709
C	-3.5138	-3.4695	-2.3834
H	-4.5991	-3.4080	-2.3179
C	-2.7718	-4.2576	-3.2340
H	-3.0807	-4.9457	-4.0207
C	3.2546	-2.2069	0.1789
H	2.8817	-2.8234	1.0011
C	4.4951	-1.5617	0.0400
H	5.3365	-1.5661	0.7314
C	4.4273	-0.9439	-1.1887
H	5.1714	-0.3674	-1.7384
Ni	0.5217	-2.5199	-1.2710

References:

(S1) Jacquart, A.; Tauc, P.; Pansu ,R. B.; Ishow, E. *Chem. Commun.*, **2010**, *46*, 4360-4362.

(S2) Wanniarachchi, S.; Liddle, B. J.; Lindeman, S. V.; Gardinier, J. R. *J. Organomet. Chem.* **2011**, *696*, 3623-3636.

(S3) Liddle, B.J.; Silva, R.M.; Morin, T.J.; Macedo, F.P.; Shukla, R.; Lindeman, S.V.; Gardinier, J.R *J. Org. Chem.* **2007**, *72*, 5637-5646.

(S4) Wanniarachchi, S.; Liddle, B. J.; Toussaint, J.; Lindeman, S. V.; Bennett, B.; Gardinier, J. R. *.Dalton Trans.* **2010**, *39*, 3167 – 3169.

(S5) Coulson; D. R.; Satek, L. C.; Grim, S. O. *Inorg. Synth*. **1990**, *28*, 107-109.

(S6) (a) Gagné, R. R.; Koval, C. A., Lisensky, G. C. *Inorg. Chem.* **1980**, *19*, 2855-2857. (b) Noviandri, I.; Brown, K. N.; Fleming, D. S.; Gulyas, P. T.; Lay, P. A.; Masters, A. F.; Phillips, L. *J. Phys. Chem. B*, **1999**, *103*, 6713-6722. (c) Bond, A. M.; Oldham, K.B.; Snook, G. A. *Anal. Chem.* **2000**, *72*, 3492-3496. (d) Bao, D.; Millare, B.; Xia, W.; Steyer, B. G.; Gerasimenko, A. A.; Ferreira, A.; Contreras, A.; Vullev, V. I. *J. Phys. Chem. A* **2009**, *113*, 1259-1267.

(S7) Bain, G. A.; Berry, J. F. *J. Chem. Ed.* **2008**, *85*, 532 – 536.

(S8) (a) Liddle, B. J.; Wanniarachchi, S.; Hewage, J. S.; Lindeman, S. V.; Bennett, B.; Gardinier, J. R. *Inorg. Chem.* **2012**, *51*, 12720-12728. (b) Wanniarachchi, S.; Liddle, B. J.; Kizer, B.; Hewage, J. S.; Lindeman, S. V.; Gardinier, J. R. *Inorg. Chem.* **2012**, *51*, 10572-10580. (c) Wanniarachchi, S.; Liddle, B. J.; Toussaint, J.; Lindeman, S. V.; Bennett, B.; Gardinier, J. R. *Dalton Trans.* **2011**, *40*, 8776-8787.

(S9) Underhill, A. E.; Billing, D. E. *Nature* **1966**, *210*, 834 – 835.

(S10) Astley, T.; Gulbis, J. M.; Hitchman, M. A.; Tiekink, E. R. T. *J. Chem. Soc. Dalton Trans.* **1993**, 509–515.

(S11) Reimann, C. W. *J. Phys. Chem.* **1970**, *74*, 561–568.

(S12) Zhao, Y.; Truhlar, D. G. *Theor. Chem. Account* **2008**, *120*, 215-241.

(S13) (a) Luo, S.; Averkiev, B.; Yang, K. R.; Xu, X.; Truhlar, D. G. *J. Chem. Theory Comput.* **2014**, *10*, 102−121. (b) Khobragade, D. A.; Mahamulkar, S. G.; Pospíšil, L.; Císarová, I.; Rulíšek, L.; Jahn, U. *Chem. Eur. J.* **2012**, *18*, 12267 – 12277. (c) Kulkarni, A. D.; Truhlar, D. G. *J. Chem. Theory Comput.* **2011**, 7, 2325-2332. (d) Zhao, Y.; Truhlar, D. G. *Acc. Chem. Res.* **2008**, *41*, 157-167.

(S14) Weigend, F. and Ahlrichs, R. *Phys. Chem. Chem. Phys.*, **2005**, *7*, 3297-3305.

(S15) Scalmani G., Frisch, M. J. *J. Chem. Phys.*, **2010**, *132*, 114110-114124.

(S16) Gaussian 09, Revision B.01, Frisch, M. J.; Trucks, G. W.; Schlegel, H. B.; Scuseria, G. E.; Robb, M. A.; Cheeseman, J. R.; Scalmani, G.; Barone, V.; Mennucci, B.; Petersson, G. A.; Nakatsuji, H.; Caricato, M.; Li, X.; Hratchian, H. P.; Izmaylov, A. F.; Bloino, J.; Zheng, G.; Sonnenberg, J. L.; Hada, M.; Ehara, M.; Toyota, K.; Fukuda, R.; Hasegawa, J.; Ishida, M.; Nakajima, T.; Honda, Y.; Kitao, O.; Nakai, H.; Vreven, T.; Montgomery, Jr., J. A.; Peralta, J. E.; Ogliaro, F.; Bearpark, M.; Heyd, J. J.; Brothers, E.; Kudin, K. N.; Staroverov, V. N.; Kobayashi, R.; Normand, J.; Raghavachari, K.; Rendell, A.; Burant, J. C.; Iyengar, S. S.; Tomasi, J.; Cossi, M.; Rega, N.; Millam, J. M.; Klene, M.; Knox, J. E.; Cross, J. B.; Bakken, V.; Adamo, C.; Jaramillo, J.; Gomperts, R.; Stratmann, R. E.;

Yazyev, O.; Austin, A. J.; Cammi, R.; Pomelli, C.; Ochterski, J. W.; Martin, R. L.; Morokuma, K.; Zakrzewski, V. G.; Voth, G. A.; Salvador, P.; Dannenberg, J. J.; Dapprich, S.; Daniels, A. D.; Farkas, Ö.; Foresman, J. B.; Ortiz, J. V.; Cioslowski, J.; Fox, D. J. Gaussian, Inc., Wallingford CT, 2009.

(S17) (a) Casida, M. E.; Jamorski, C.; Casida, K. C.; Salahub, D. R. *J. Chem. Phys.*, **1998**, *108*, 4439-4449. (b) Scalmani, G.; Frisch, M. J.; Mennucci, B.; Tomasi, J.; Cammi, R.; Barone, V. *J. Chem. Phys.*, **2006**, *124*, 094107: 1-15.

(S18) Noodleman, L. *J. Chem. Phys.* **1981**, *74*, 5737-5743.

(S19) (a) Kelly, C. P.; Cramer, C. J.; Truhlar, D. G. *J. Phys. Chem. B* **2007**, 111, 408−422 (b) Winget, P.; Cramer, C. J.; Truhlar, D. G. *Theor. Chem. Acc.* **2004**, *112*, 217−227.

(S20) Rulíšek, L. *J. Phys. Chem. C* **2013**, *117*, 16871−16877.